Rogers, Alistair; Medlyn, Belinda E.; Dukes, Jeffrey S.; Bonan, Gordon; von Caemmerer, Susanne; Dietze, Michael C.; Kattge, Jens; Leakey, Andrew D.B.; Mercado, Lina M.; Niinemets, Ulo; Prentice, I. Colin; Serbin, Shawn P.; Sitch, Stephen; Way, Danielle A.; Zaehle, Sonke. 2017. **A roadmap for improving the representation of photosynthesis in Earth system models.** *New Phytologist*, 213 (1). 22-42. 10.1111/nph.14283

A Roadmap for Improving the Representation of Photosynthesis in Earth System Models

Alistair Rogers[1], Belinda E. Medlyn[2], Jeffrey S. Dukes[3], Gordon Bonan[4], Susanne von Caemmerer[5], Michael C. Dietze[6], Jens Kattge[7,8], Andrew D.B. Leakey[9], Lina M Mercado[10,11], Ülo Niinemets[12] I. Colin Prentice[13,14,15], Shawn P. Serbin[1], Stephen Sitch[10], Danielle A. Way[16], Sönke Zaehle[17]

[1]Environmental and Climate Sciences Department, Brookhaven National Laboratory, Upton, NY 11973-5000, USA

[2]Hawkesbury Institute for the Environment, University of Western Sydney, Locked Bag 1797, Penrith NSW 2751, Australia

[3]Department of Forestry and Natural Resources and Department of Biological Sciences, Purdue University, West Lafayette, IN 47907-2061, USA

[4]National Center for Atmospheric Research, Boulder, CO 80307-3000, USA

[5]Research School of Biology, College of Medicine, Biology and the Environment, Linnaeus Building (Bldg 134) Linnaeus Way, The Australian National University, Canberra ACT 0200 Australia

[6]Department of Earth and Environment, Boston University, Boston, MA 02215, USA

[7]Max Planck Institute for Biogeochemistry, 07701, Jena, Germany.

[8]German Centre for Integrative Biodiversity Research (iDiv) Halle-Jena-Leipzig, Deutscher Platz 5e, 04103 Leipzig, Germany

[9]Department of Plant Biology and Institute for Genomic Biology, University of Illinois at Urbana-Champaign, IL 61801, USA

[10]Geography Department, College of life and Environmental Sciences, University of Exeter, Exeter, EX4 4SB, UK

[11] Centre for Ecology and Hydrology, Wallingford, OX10 8BB, UK

[12]Department of Plant Physiology, Estonian University of Life Sciences, Kreutzwaldi 1, 51014 Tartu, Estonia

[13]AXA Chair of Biosphere and Climate Impacts, Grand Challenges in Ecosystems and the Environment and Grantham Institute for Climate Change, Department of Life Sciences, Imperial College London, Silwood Park Campus, Buckhurst Road, Ascot SL5 7PY, UK

[14]Department of Biological Sciences, Macquarie University, North Ryde, NSW 2109, Australia

[15]State Key Laboratory of Soil Erosion and Dryland Farming on the Loess Plateau, College of Forestry, Northwest Agriculture & Forestry University, Yangling 712100, China

[16]Department of Biology, University of Western Ontario, London, ON, Canada, N6A 5B7 and Nicholas School of the Environment, Duke University, Durham, NC, USA 27708

[17]Biogeochemical Integration Department, Max Planck Institute for Biogeochemistry, Hans-Knöll-Str. 10, 07745 Jena, Germany

Corresponding Author
Alistair Rogers
Environmental and Climate Sciences Department
Brookhaven National Laboratory
Upton, NY 11973-5000
USA
arogers@bnl.gov
+1 631 344 2948

Section	Word Count
Main Body	9912
Introduction	554
Representation of Leaf photosynthesis in Terrestrial Biosphere Models	5472
Scaling physiology	3575
Conclusion	320
Acknowledgements	100
Number of Figures	6 (all in color)
Number of Tables	2
Supporting Information	0

Summary

- Accurate representation of photosynthesis in terrestrial biosphere models (TBMs) is essential for robust projections of global change. However, current representations vary markedly between TBMs, contributing uncertainty to projections of global carbon fluxes.
- Here we compared the representation of photosynthesis in seven TBMs by examining leaf and canopy level responses of *A* to key environmental variables: light, temperature, carbon dioxide concentration, vapor pressure deficit and soil water content.
- We identified research areas where limited process knowledge prevents inclusion of physiological phenomena in current TBMs and research areas where data are urgently needed for model parameterization or evaluation.
- We provide a roadmap for new science needed to improve the representation of photosynthesis in the next generation of terrestrial biosphere and Earth System Models.

Key Words: carbon dioxide, light, stomatal conductance, soil water content, temperature, terrestrial biosphere models, vapor pressure deficit.

Introduction

Fossil energy use is the dominant driver of the increase in atmospheric CO_2 concentration (C_a) and the principal cause of global climate change (IPCC, 2013). Many of the observed and projected impacts of rising C_a portend increasing environmental and economic risk, yet the uncertainty surrounding the projection of our future climate by Earth System Models (ESMs) is unacceptably high (Friedlingstein *et al.*, 2006, Friedlingstein *et al.*, 2014).

Although CO_2 emissions associated with anthropogenic activity are notable (11 Pg C $year^{-1}$), they represent less than 10% of the gross carbon fluxes between the land surface and the atmosphere (Beer *et al.*, 2010, Boden *et al.*, 2013, Le Quéré *et al.*, 2015). Terrestrial photosynthetic CO_2 assimilation (A) is the largest of these CO_2 fluxes (~120 Pg C $year^{-1}$), subsidizing our use of fossil fuels through the net assimilation of about one-third of the CO_2 emissions associated with anthropogenic activities (Le Quéré *et al.*, 2015). However, there is critical uncertainty about how the terrestrial carbon sink will be affected by changes in A with rising C_a, temperature and drought (Friedlingstein *et al.*, 2014, Gregory *et al.*, 2009, IPCC 2013). Therefore, reducing the uncertainty associated with model representation of A is an essential part of improving confidence in projections of global change (Ciais *et al*., 2013).

In this study we have focused on photosynthesis, but recognize that improving the understanding and projection of the terrestrial biosphere's response to global change also depends on realistically representing many additional processes that are down stream of carbon assimilation (e.g. carbon allocation, plant and soil respiration, and nutrient cycling). Of

87 particularly relevance to photosynthesis is the allocation of extra carbon to leaf area in trees
88 grown at elevated C_a (Ainsworth & Long, 2005). Model representation and integration of these
89 processes, and how the balance between them shifts in their individual and combined
90 responses to environmental drivers, will also be critical in order to capture whole system
91 responses, but such a comprehensive discussion is beyond the scope of this study.
92
93 We examined model representations of *A* in seven Terrestrial Biosphere Models (TBMs). These
94 models include four that represent the land component of ESMs which were part of the recent
95 Coupled Model Intercomparison Project (CMIP5) - the main resource for the IPCC Fifth
96 Assessment Report (Friedlingstein *et al.*, 2014, IPCC, 2013). Our approach focuses on how
97 physiological responses are represented by TBMs. We compared modeled responses of *A* to
98 key environmental variables in order to identify areas of model divergence that reflect gaps in
99 current understanding of the physiological and environmental controls of *A*. In the second half
100 of the paper, we turn to issues of scale - vertical, horizontal and temporal - and consider how
101 representation and parameterization of leaf-level processes is scaled to the canopy within
102 current model frameworks.
103
104 We had three goals: (1) understand how models differ in their representation of *A*; (2) identify
105 gaps in current understanding of *A* that contribute to uncertainty in model output; (3) identify
106 areas where current process knowledge and emerging data sets can be used to improve model
107 skill. This study provides recommendations for immediate improvements that can be made to

current model representation of *A* and also highlights the scientific activity needed to further advance representation of *A* in the next generation of TBMs.

Representation of Leaf Photosynthesis in Terrestrial Biosphere Models

Current model structure and parameterization

The Farquhar, von Caemmerer and Berry (FvCB) model of *A* (Farquhar *et al.*, 1980, von Caemmerer, 2000, von Caemmerer & Farquhar, 1981) provides a robust mechanistic representation of *A* in C_3 species, and is the foundation for model estimation of gross primary production (GPP) in many TBMs (Cramer *et al.*, 2001, Rogers, 2014), including the seven models considered here (BETHY, CLM, ED2, G'DAY, JSBACH, JULES and O-CN; Table 1). The formulations of the FvCB model used in these TBMs include elements of; Collatz *et al.* (1991), in CLM, ED2 and JULES; Foley *et al* (1996), in ED2; and Kull & Kruijt (1998), in O-CN (Table 1). The FvCB model represents photosynthetic CO_2 assimilation as the most limiting of two biochemical processes: Rubisco carboxylation, and ribulose-1,5-bisphosphate (RuBP) regeneration driven by electron transport. These processes limit *A* in most environments; however, Sharkey (1985) subsequently described how limitations on triose phosphate utilization (TPU limitation) could also limit *A* under some conditions. Only two models in this study included TPU limitation (CLM and JULES, Table 1).

129 Similar biochemical models have been developed for the C_4 photosynthetic pathway (von
130 Caemmerer et al. 2000). For reasons of space, we limit our discussion to model treatment of C_3
131 photosynthesis. However we note that a similar exercise focused on C_4 photosynthesis would
132 be valuable.
133
134 Models typically represent stomatal conductance (g_s) using a coupled relationship with *A* that
135 varies with atmospheric, or leaf-surface, CO_2 concentration, and some measure of atmospheric
136 humidity. This model approach was originally formulated by Ball *et al*. (1987), who used a direct
137 dependence on relative humidity (*RH*) in their equation for g_s. Ball *et al*.'s equation is still
138 widely used in many TBMs, including CLM. Leuning (1995) suggested an alternative equation
139 that depends on vapor pressure deficit (*VPD*) rather than *RH*. ED2 uses the Leuning (1995)
140 equation, while JULES uses a very similar equation developed by Jacobs (1994). The approaches
141 to represent g_s implemented by the models considered here are quite diverse (Table 1) which
142 has a wide-ranging impact on the model outputs we considered.
143
144 The TBMs in this study represent vegetation using broad plant functional types (PFTs). The
145 FvCB model is parameterized with a number of important constants that are typically the same
146 for all PFTs. PFTs are distinguished with respect to photosynthesis through differences in the
147 estimates of the maximum carboxylation rate of Rubisco ($V_{c,max}$), the maximum rate of electron
148 transport (J_{max}) and the slope of the stomatal conductance response. Several groups are now
149 working towards next-generation vegetation models in which PFTs are replaced by "trait-based
150 approaches" (Wullschleger *et al.* 2014). This catchall phrase includes leveraging trait-

151 environment linkages (Ali et al. 2015, Reich 2014, van Bodegom et al. 2014), optimality
152 approaches (Xu et al. 2012, Meir et al. 2015), trait filtering (Fisher et al. 2012) and adaptive
153 global vegetation models (Scheiter et al. 2013). However, our review is relevant to these
154 approaches as well, as they still employ similar representations of photosynthesis. The key
155 difference lies in parameterization, which we discuss when considering scaling to landscapes.
156
157 **Mesophyll conductance**
158
159 In C_3 species, mesophyll conductance (g_m) describes the conductance to CO_2 diffusion from the
160 intercellular airspace within a leaf to the sites of carboxylation within chloroplasts (Flexas *et al.*,
161 2012, von Caemmerer & Evans, 1991). It is one of the four main physiological processes limiting
162 CO_2 uptake and fixation, the others being g_s and the biochemical activity of Rubisco and RuBP
163 regeneration. To our knowledge, there are no land models that currently contribute to the IPCC
164 assessments that consider g_m. This absence reflects the challenge of adding further complexity
165 to the models, but also the uncertainty and technical difficulty of the measurements required
166 to estimate g_m.
167
168 Response curves of A to intercellular [CO_2] (C_i) are routinely used to infer the maximum
169 biochemical activity of Rubisco and RuBP regeneration, i.e. $V_{c,max}$ and J_{max}. When the FvCB
170 model was conceived, the assumption was made that the difference between C_i and the [CO_2]
171 within the chloroplast (C_c) was sufficiently small that it could be ignored. Subsequently,
172 improved measurement techniques for g_m have shown that it can impose a significant

limitation on *A* which varies with temperature, and there are significant species differences in these responses (von Caemmerer & Evans, 2015). If g_m is not taken into account in the analysis of *A*-C_i curves, the true $V_{c,max}$ will be underestimated (Niinemets *et al.*, 2009, Sun *et al.*, 2014, von Caemmerer, 2000). Furthermore, temperature responses of $V_{c,max}$ and J_{max} derived from gas exchange measurements will not necessarily reflect the temperature dependence of the underlying biochemistry alone, but will also reflect the temperature response of g_m (Medlyn *et al.*, 2002a). The use of apparent parameters is problematic if modelers wish to incorporate new data on the underlying biochemistry of photosynthesis. For example, a recent biochemical survey of the catalytic diversity in Rubisco revealed significant and marked variation in key parameters across 75 species (Orr *et al*. 2016). These data cannot be used directly in models without including g_m in model structures, highlighting the need for improved understanding and model representation of g_m.

Several TBMs currently use linear relationships between apparent $V_{c,max}$ (obtained from *A*-C_i curves) and leaf nitrogen to derive $V_{c,max}$ prognostically. If g_m were to be incorporated into future TBMs, new algorithms linking $V_{c,max}$ to leaf N content would be required as the $V_{c,max}$ used in the relationship would need to be derived as a function of C_c not C_i. Currently a reliance on apparent V_{cmax} - leaf N relationships means that models underestimate the amount of N partitioned to Rubisco, or put another way, overestimate the nitrogen use efficiency of CO_2 carboxylation by Rubisco.

It is clear that an improved understanding of g_m remains a critical research area. Despite recent important progress that may simplify prediction of g_m (Tholen *et al.* 2012), we feel that immediate inclusion of g_m in TBMs is premature. "Apparent" parameters derived from A-C_i response curves, which implicitly account for g_m, have been used successfully to model A in many ecosystems at the leaf and canopy level (e.g. Bernacchi *et al*. 2003; Medlyn *et al*. 2005; Thum *et al*. 2007). Until understanding and measurement of g_m matures, its inclusion in TBMs will likely drive additional uncertainty. Furthermore, the modeling community currently has access to a substantial dataset (albeit heavily biased to the mid-latitudes) of "apparent" parameters but almost no data for $V_{c,max}$ and J_{max} derived from A-C_c curves. Including g_m now would dramatically shrink the amount of data available for model parameterization. However, it is important to note that inclusion of g_m in models is essential if carbon isotope discrimination is to be inferred (Ethier & Livingston, 2004; Suits *et al.* 2005).

Recommendation: (1) Greater process knowledge of g_m will be required before it can be included in TBMs. Specific needs include improved understanding of variation in g_m across PFTs and how it is affected by environmental drivers such as light and temperature.

Short-term leaf level responses to environmental variables in current model structures

Our goal was to understand and compare the physiological responses inside these seven TBMs (Table 1). We focused on one particular PFT - a broad leaved deciduous tree - and defined several environmental and physiological variables which provided standard conditions for model intercomparison: instantaneous quantum flux density (Q) = 1500 μmol mol^{-1}, upper

canopy sunlit leaf temperature = 25°C, C_a = 380 µmol mol^{-1}, [O_2] = 210 mmol mol^{-1}, *VPD* = 1 kPa, soil moisture content at field capacity and $V_{c,max}$ = 60 µmol m^{-2} s^{-1}. In the following sections we present and discuss leaf level responses to light, temperature, C_a, *VPD* and soil water content.

Short-term response to light

The initial slope of the photosynthetic light response curve is determined by the maximum quantum yield of CO_2 assimilation. For clarity, here we distinguish between the *intrinsic* quantum yield (Φ_{int}), which is the initial slope of the relationship between *A* and absorbed *Q* under non-photorespiratory conditions and the *realized* quantum yield (Φ_{real}), which we define as the photosynthetic rate per unit incident light at *Q* = 100 µmol m^{-2} s^{-1} in our standard conditions (Table 2 and the initial slope of the *A*-*Q* response in Fig. 1a). The Φ_{int} is generally an input parameter to the models (Table 2) whereas the realized quantum yield is calculated by the models using the FvCB equations, and depends not only on the Φ_{int} but also on the assumed values for the Rubisco kinetic constant Γ^* (the CO_2 compensation point in the absence of mitochondrial respiration), the low light C_i, the leaf absorptance (a), and the convexity of the light response curve (Θ). Model variation in the choice of kinetic constants, low light C_i, a and Θ are summarized in Table 2. The CLM model assumes that Φ_{int} is equal to the theoretical maximum of (1-f)/8, where f=0.15 and is used to correct for the spectral quality of light (von Caemmerer, 2000). As a result, CLM has the highest Φ_{real} (0.053 mol mol^{-1}, Table 2, Fig. 1a). The other models are parameterized with quantum yield inputs that result in a calculated Φ_{int}

238 that is below the theoretical maximum and the resulting values for Φ_{real} are lower than those
239 for CLM (Table 2). Despite a parameterization that is broadly consistent with other models, the
240 initial slope of the *A*-*Q* response of O-CN is strikingly low and results from a limitation of *A* by
241 light harvesting at low *Q* (Kull & Kruijt, 1998; Table 1).
242
243 Experimental studies focused on understanding natural variation in quantum yield have shown
244 that there is little variation in Φ_{int} under unstressed conditions across a wide range of species,
245 with an average value of 0.092 mol mol^{-1} (Long *et al*. 1993; Singsaas, Ort & DeLucia, 2001),
246 comparable with the range of Φ_{int} used in the models considered here (0.07 – 0.106, Table 2).
247 However, Φ_{int} can be substantially lower in the field, particularly in stressed conditions (Medlyn
248 *et al* 2007; Niinemets *et al*. 2004, 2014; Singsaas, Ort & DeLucia, 2001). As discussed above, the
249 Φ_{real} in models depends on several assumptions, not just the Φ_{int}, highlighting the need to
250 better parameterize and test modelled light responses with data from field conditions. For
251 example, most existing measurements have been made within a narrow temperature range (20
252 – 30°C) and the scarcity of data collected at low temperature has been highlighted as an
253 important driver of model uncertainty at high latitudes (Dietze *et al*., 2014).
254
255 Leaf level light-saturated CO_2 uptake (A_{sat}) varies considerably between models (Fig 1a). The
256 variation in modelled A_{sat} is driven by differences in prescribed Rubisco kinetic constants and
257 their temperature dependencies (see below and Table 2), as well as the C_i, which is dependent
258 on the choice of stomatal model. The inflection point of the light response curve marks the
259 transition between light limitation and light saturation of *A*. There is a wide range in the *Q* at

which *A* becomes light saturated and therefore the greatest model divergence in *A* occurs when some models have light saturated *A* and others do not (i.e. Q = 400-800 µmol m^{-2} s^{-1}, Fig. 1). In addition to differences in the model representation of light limited and light saturated *A,* variation in the transition phase is attributable to model structure (Table 1), and when present, parameterization of the convexity term (Θ, Table 2), which determines the relative influence of Φ_{real} or A_{sat} on *A* at a given *Q*.

Moving from the leaf to the canopy level, responses to irradiance (Fig 1, b-d) are not only dependent on the factors discussed above but also on the method used to scale physiology from the leaf to the canopy level, the representation of the light environment within the canopy, and the partitioning of foliage between sunlit and shaded leaves (Gu *et al.* 2002, Mercado *et al.* 2009). As a result, canopy scaling exacerbates existing differences between the TBMs and introduces new structural variation that further diversifies model output (Fig. 1 b-d). Canopy scaling is discussed in detail below.

Recommendation: (2) Modeled responses of photosynthesis to light need to be parameterized and evaluated against data from field conditions, particularly at low temperature.

Don't mix & match

One issue that emerged here, but is relevant throughout this paper, is the need to avoid piecemeal approaches to model parameterization. For example, we need to carefully and consistently use kinetic constants and temperature response functions because the models are highly sensitive to them. Any constants and functions used when deriving photosynthetic

parameters from data have to be the *same ones* used in the model. For example, if a value of $V_{c,max}$ at 25°C is used in a model, that model must use the same Michaelis-Menten constants (K_c and K_o) and Γ^* (e.g. see Table 2), and the associated temperature dependencies, that were used to estimate $V_{c,max}$ from the original A-C_i response curve as well as the same temperature response function (e.g. see Table 1) used to scale $V_{c,max}$ from the measurement temperature to 25°C. This problem, that derived parameters depend on the equations used to derive them, introduces error when trying use the parameters to perform meta-analyses or calibrate models (Medlyn *et al*. 2002, Dietze 2014). As we make progress to provide models with richer data sets for use in model parameterization and evaluation, we need to archive our raw gas exchange data so that, for example, new kinetic constants and temperature response functions can be applied to old data, maintaining its value as understanding advances. The estimation of quantum yield provides another example where the assembly of parameters (e.g. Φ_{int}, a, Γ^*, Θ) and approaches (e.g. estimation of low light C_i) is not coordinated and where archived data would be useful.

Recommendations: (3) Models need to make careful and consistent use of kinetic constants and temperature response functions. (4) Physiologists should archive their raw data to enable coordinated parameterization and the preservation of their data for future analysis.

Short-term response to temperature

The temperature response of A is complex and dependent on additional variables such as Q and C_i (Fig 2). The C_i in turn depends on g_s and hence *VPD*, such that the temperature and *VPD*

response of g_s also impacts the shape of the temperature response of *A* (Medlyn *et al*., 2002a; Lin *et al*., 2012). The model by Farquhar *et al*. (1980) suggests that *A* is Rubisco-limited at low temperature - but note that TPU limitation can limit *A* in some species at low temperature (Sage & Sharkey, 1987). The decline in *A* at high temperature (Fig. 2) can be brought about by the temperature dependence of J_{max} and the strong increase in photorespiration and mitochondrial respiration with increasing temperature (Farquhar *et al*., 1980; von Caemmerer, 2000). High temperature limitations on Rubisco activase could also cause decline in *A* but this mechanism is currently absent from all these models (Salvucci & Crafts-Brandner 2004a; Salvucci & Crafts-Brandner 2004b, Sage & Kubien 2007). The steep decline of *A* at temperatures above 30°C in the Farquhar *et al.* (1980) model is largely driven by the temperature dependence of J_{max}. This effect needs to be treated with some caution as it may be due to irreversible inhibition in the *in vitro* system, from which the function was derived. June *et al*. (2004) provided a simpler empirical equation for fitting the temperature dependence of J_{max}. The temperature dependence of *A* is also driven by the choice of kinetic parameters and their temperature dependencies as discussed above. Some TBMs use spinach (Jordan and Ogren 1984) or tobacco (Bernacchi *et al*. 2001) temperature response functions for $V_{c,max}$ for all species. However, as there are important differences in the response of $V_{c,max}$ to temperature among warm and cool climate plant species (Kattge & Knorr 2007; Galmes *et al*. 2015), continued acquisition of temperature response functions from different biomes is critically important. The temperature optimum of *A* (T_{opt}) depends on environmental conditions such as *Q* and C_a, with T_{opt} being more pronounced at high *Q* and C_a (e.g. compare Figs 2a & c with 2b & dd). Here, two models stand out for their temperature responses; unlike the majority of

models that show an optimum ~24.5°C, ED2 has an emergent temperature optimum at 16°C, despite a $V_{c,max}$ optimum at 39°C, and JSBACH shows no high temperature limitation on A (Table 1, Fig 2). It is usual for T_{opt} to shift to a slightly higher temperature as C_a rises (Long, 1991) because at high C_a the rate of photorespiration is reduced, thereby extending the temperature range where positive CO_2 assimilation occurs. The CO_2 effect on T_{opt} is evident in Fig. 2 in a number of the models at both the leaf and canopy level. Here, elevating C_a from 380 to 550 µmol mol^{-1} shifts the T_{opt} up by ~2°C (Fig 2 b,d). Two models do not show this shift in T_{opt}: JSBACH has no T_{opt}, and the T_{opt} for ED2 remains at 16°C despite the increase in C_a from 380 to 550 µmol mol^{-1}.

Current empirical models predict the response of g_s to temperature based on a relationship between g_s and A that is modified by VPD. This approach is successful in many cases (e.g. Duursma *et al*. 2014) although the mechanisms underlying the response remain poorly understood (Mott, 2009; Busch, 2013). In addition, there is evidence that the correlation between g_s and A breaks down at high temperatures (> 35°C) in some species, with stomata remaining open while A goes to zero (e.g. Lu *et al*. 2000; Scafaro *et al*. 2012; Slot *et al*. 2016; Teskey *et al*. 2015; von Caemmerer and Evans 2015). Presumably this response allows the plant to maintain leaf temperatures at non-damaging levels via transpirational cooling. It is not known how widespread this response is (Teskey *et al*. 2015) nor to what extent it occurs in the field. Slot *et al*. (2016), for example, find this response in glasshouse-based measurements but not in field trees.

Recommendations: (5) Physiologists need to continue measuring temperature response functions for $V_{c,max}$ and J_{max}. (6) More field-based research into the independent temperature response of g_s is required to better understand the mechanism underlying the response of A to high temperatures.

Short-term response to CO_2

At low C_a, when *A* is limited by the amount of active Rubisco available for carboxylation ($V_{c,max}$), *A* increases with rising C_a for two reasons: (1) the affinity of Rubisco for CO_2 is low, and therefore increasing the substrate concentration increases carboxylation rates; (2) CO_2 competitively inhibits the oxygenation reaction, reducing CO_2 losses associated with photorespiration (Fig. 3). At higher C_a - i.e. above the inflection point of the A-C_a curve (most notable in the leaf level responses shown in Figs 3a & b) - *A* becomes limited by the supply of ATP and NADPH to regenerate the CO_2 acceptor RuBP. At this point *A* will still rise with increasing C_a, but the CO_2 responsiveness (the increase in *A* for a given increase in C_a) is reduced as further increases in *A* are attributable solely to the inhibition of the oxygenation reaction, which increases the availability of ATP and NADPH for RuBP regeneration (Long 1991, Long *et al.* 2004).

The shape of the *A*- C_a response curve is a critical model feature that determines the ability of the terrestrial carbon sink to respond to rising C_a and it is affected by model structure and parameterization (Fig. 3, Tables 1 & 2). Variation in the initial slope of the *A*-C_a response is

attributable to C_i and the choice of kinetic constants. For this example of a broad leafed deciduous tree PFT in our standard conditions, all models show that light-saturated *A* appears to be Rubisco limited (RuBP saturated) below a C_a of 500 µmol mol^{-1} (Fig. 3). As a result the CO_2 responsiveness of *A* below a C_a of 500 µmol mol^{-1} is similar for all models. However, as C_a rises above 500 µmol mol^{-1} differences in model structure and parameterization lead to substantial variation in CO_2 responsiveness. Three models (CLM, ED2 and JULES) stand out for smooth response curves that lack a clear inflection point (most noticeable in Fig 3a). All three models adopt the co-limitation approach described by Collatz *et al*. (1991) which smooths transitions between Rubisco limited and RuBP limited *A* (Collatz *et al.* 1991; Foley *et al*. 1996; Clark *et al*. 2011; Oleson *et al*. 2013, Table 1). This approach contributes to the greater CO_2 responsiveness at higher C_a observed in CLM and JULES (Fig 3a). In addition, the four models that lack this smoothing function (BETHY, G'DAY, JSBACH and O-CN) have a marked inflection point between Rubisco limited and RuBP limited *A*, but the C_a at which this inflection occurs spans a large range (~300 µmol mol^{-1}, Fig. 3) contributing to the variation in CO_2 responsiveness above 500 µmol mol^{-1}. The variation in C_a at which the inflection point occurs has several causes, but the main drivers of this variation are the choice of kinetic constants (~60 µmol mol^{-1}, Table 2), the JV_{ratio}, which for a fixed $V_{c,max}$ sets the inflection point C_i (~125 µmol mol^{-1}, Table 2) and the stomatal model, which determines the C_a at which the inflection point C_i is reached (~175 µmol mol^{-1}, Table 1).

As $V_{c,max}$ is reduced (Fig. 3b, 3d), the responses of *A* to changes in C_a are qualitatively similar but model divergence is constrained. Model variation in canopy level responses to rising C_a (Fig

3c & d) is also attributable to different approaches to canopy scaling as discussed below. The differences seen here in CO_2 responsiveness are substantial - highlighting the impact of different model representations of the FvCB equations, stomatal model choices and the need to better understand controls on the inflection point of the A-C_a response. The C_a at which the inflection point occurs drives uncertainty in the CO_2 stimulation of *A* at the C_a that will be experienced in the second half of the century, and it is at this higher C_a where model uncertainty is greatest. This effect probably contributes to the model differences in *GPP* reported in the recent FACE model-intercomparison project (Zaehle *et al.* 2014).

Recommendation: (7) We need improved understanding and model evaluation of the controls on the inflection point of CO_2 response curves.

Short-term response to VPD

Increasing *VPD* causes stomatal closure, which decreases C_i . The magnitude of the decrease in *A* resulting from lower C_i is determined by the shape of the *A*-C_i response as described above and shown in Fig. 3. Figure 4 shows the response of *A* to *VPD;* model divergence increases with rising *VPD*, largely due to differences in the parameterization of *VPD* sensitivity among models . The strong sensitivity of the CLM model seen in Figure 4 is due to the use of *RH* in the model formulation, and the fact that RH must drop dramatically to obtain increasing *VPD* with constant temperature, as shown in this plot. There are some models, of which JSBACH in this study is an example, that do not incorporate a stomatal response to *RH* or *VPD* (Table 1, Figure 4). Such formulations were necessary when driving data sets for atmospheric humidity were not available. Given advances in the understanding of stomatal responses and the availability

of appropriate driver datasets, stomatal response to *RH* or *VPD* should be adopted. However, we believe that formulations involving *VPD*, such as those adopted by ED2, G'DAY and JULES (Table 1) are theoretically preferable because, unlike *RH*, *VPD* is directly proportional to water loss, more closely reflects stomatal mechanics (e.g. Aphalo & Jarvis 1991; de Beeck, 2010), and is strongly linked to productivity (Lobell *et al*. 2014; Ort & Long, 2014). In addition, formulations involving *VPD,* rather than *RH,* will likely be better able to project the response of vegetation to future climate scenarios, because *RH* is predicted to change little in the future whereas *VPD* will increase with warming (Sato *et al*. 2015).

Similar coupled g_s-*A* models can also be developed from optimization principles. Cowan & Farquhar (1977) proposed that stomatal behavior is optimal when *A* less the cost of transpiration is maximized, and a number of authors have shown that this theory leads to a relationship between g_s and *A* that is similar in behavior to empirical formulations (e.g. Hari *et al*. 1986; Katul *et al*. 2010; Medlyn *et al*. 2011). Optimization approaches have the advantage of being based in theory, yielding meaningful parameter values, and providing g_s responses to future environmental conditions where we lack robust measurements, and we encourage their use. However, we also caution that optimization can lead to physiologically incorrect behavior in some circumstances – such as incorrect CO_2 responses, and instability near the transition between Rubisco-limited and RuBP regeneration-limited *A* – implying that simple, empirically verified equations based on optimization may be more reliable than direct application of numerical optimizations that are also dependent on the careful application of model constraints within TBMs and the optimization approach used.

435

436 Large-scale parameterization of stomatal models has been data-limited, with models typically
437 using one nominal set of parameter values for all C_3 vegetation. A major advance in this area
438 was made by Lin *et al*. (2015), who collated a substantial new stomatal conductance database
439 and demonstrated a predicted response of the stomatal slope parameter (g_1) to temperature
440 and consistent differences in g_1 among broadly defined PFTs. This dataset provides a valuable
441 foundation for stomatal model parameterization. However, the coverage of this database is still
442 limited. There is still relatively little information about how g_1 varies among species or
443 genotype, and almost no information on acclimation or plasticity in these parameters in
444 response to abiotic or biotic factors (Way *et al*. 2011). Models are also sensitive to the
445 minimum stomatal conductance parameter, g_0, particularly under low light and high *VPD*
446 conditions (Bauerle *et al*. 2014), but this parameter is poorly quantified.
447 *Recommendation: (8) Models should adopt approaches that include formulations where g_s*
448 *responds to VPD. (9) We need more information about how g_1 and g_0 (or their equivalents) vary*
449 *among PFTs and in response to environmental drivers.*
450

451 **Short-term response to Soil Moisture Content**

452

453 Soil moisture availability is a key constraint on *A*. As soil moisture availability decreases,
454 stomates close, decreasing C_i, and eventually preventing *A* and transpiration (Fig. 5). Drought
455 can also reduce the biochemical capacity for *A*, expressed as lower $V_{c,max}$ and J_{max} in models,
456 but the relative balance of these stomatal and biochemical limitations is subject to significant

457 debate (Chaves *et al* 2009). Current approaches to modelling the effects of soil moisture on *A*
458 can be classified into several types: empirical reduction factors; hydraulic limitations;
459 physiological approaches; and a simple supply constraint approach (BETHY). The latter assumes
460 that plant transpiration cannot exceed the potential supply of soil water and that plants can
461 photosynthesize provided there is a sufficient water supply (Table 1).
462
463 The empirical reduction factor approach involves multiplying parameters by a soil water stress
464 factor (typically denoted β, ranging from 0 to 1) when soil moisture falls below a given model
465 model-dependent threshold. Three of the models in our sample used this approach (CLM,
466 G'DAY and O-CN, Table 1 & Fig. 5). However, there is disagreement among models as to
467 whether the β factor should be applied to the stomatal slope parameter, apparent $V_{c,max}$, or
468 both (De Kauwe *et al*. 2013). Here, all three models applied the β factor to stomatal model
469 parameters, either the slope (G'DAY and O-CN) or the intercept (CLM), and also to the
470 photosynthetic parameters $V_{c,max}$ (CLM) or $V_{c,max}$ and J_{max} (G'DAY and O-CN, Table 1). Increasing
471 evidence suggests that both stomatal slope and $V_{c,max}$ are affected by low soil moisture, with
472 the reduction in apparent $V_{c,max}$ possibly in part due to lower g_m (Keenan *et al*. 2010; Egea *et al*.
473 2011; Zhou *et al*. 2013). Several TBMs do include both limitations, but the β factor is tied to the
474 soil water content and therefore models cannot capture the impact of potentially different
475 trajectories of drying and rewetting episodes (Williams *et al*. 2009).
476
477 The hydraulic approach offers a number of theoretical advantages over the β-factor approach.
478 Stomatal conductance is modelled as a function of leaf water potential (ψ_{leaf}), which is

479 calculated from soil moisture potential ψ_{soil} and plant and soil hydraulic conductances. There
480 may be a threshold minimum ψ_{leaf} (Williams *et al*. 1996) or a sigmoidal functional dependence
481 (Tuzet *et al*. 2003). Implementations also differ on whether responses to *VPD* are captured by
482 the responses to ψ_{leaf} (Williams *et al*. 1996, Tuzet *et al*. 2003) or whether an additional *VPD*
483 response is also needed (Bonan *et al*. 2014). The hydraulic approach is appealing to plant
484 physiologists because it reflects some of the key mechanisms thought to influence plant
485 response to drought (Leuning *et al*. 2004). Because soil hydraulic conductance is assumed to
486 vary with ψ_{soil} this approach also incorporates a dynamic weighting of soil layers whereby lower
487 soil layers become more important as drought progresses (De Kauwe *et al*. 2015). Furthermore,
488 there is evidence that the photosynthetic response to soil moisture can depend on plant leaf
489 area (e.g. Kelly *et al*. 2015), an effect that is captured by the hydraulic approach but not the β-
490 factor approach. The chief disadvantage of the hydraulic approach is that it requires additional
491 parameters to represent plant hydraulic conductance and stomatal dependence on leaf water
492 potential. These parameters are not well quantified and can lead to additional uncertainty.
493
494 The physiological approaches are based on an understanding of stomatal function and suggest
495 that both metabolic and hydraulic stomatal regulation involves the hormone abscisic acid
496 (*ABA*), known to promote tolerance against abiotic stress (Jones *et al.*, 2015). Wilkinson and
497 Davies (2002) proposed a coordinated model of plant responses to stress whereby water stress
498 sensed by the root system stimulates *ABA* biosynthesis. This signal is then communicated to the
499 guard cells which subsequently induce stomatal closure and reduce water loss. Both roots and

500 leaves synthesize *ABA* and increasing concentrations of xylem *ABA* correlate with stomatal
501 closure (Sauter *et al.*, 2001; Wilkinson and Davies, 2002, Christmann *et al*. 2007).
502
503 There are few mathematical descriptions of stomatal control including xylem *ABA* signaling
504 (Tardieu and Davies, 1993; Dewar, 2002; Huntingford *et al.*, 2015). Tardieu and Davies (1993),
505 combined hydraulic and chemical signaling control of stomatal functioning. The approach of
506 Dewar (2002) is an extension of this approach that also considers xylem embolism and the
507 possible role of combined leaf hydraulic and chemical signaling in addition - or as a possible
508 alternative - to existing root signals. Huntingford *et al.* (2015) revisited the work by Dewar
509 (2002) and provided a g_s formulation which depends on only four variables: soil water content,
510 C_a, evapotranspiration and net *A*. This is an exciting approach, however there is an acute need
511 for more empirical data to be able to parameterize and evaluate approaches of estimating g_s
512 that include *ABA*.
513
514 The TBMs presented here showed dramatic divergence in the response of *A* to drought (Fig. 5),
515 with the canopy level responses mostly mirroring the responses seen at the leaf level. Whilst
516 much of this divergence could be explained by the different approaches taken by each model
517 (Table 1), the method used to estimate soil water availability also varies between models. Some
518 models estimate soil water availability using soil moisture content (e.g. O-CN) and others using
519 ψ_{soil} (e.g. CLM). Since soil water retention curves are highly nonlinear and dependent on soil
520 type, this can be a major source of model divergence (Medlyn *et al.* 2016). From a physiological
521 perspective, ψ_{soil} is thought to be more relevant to plant function than soil moisture content.

However, the use of ψ_{soil} can result in unrealistically steep responses to the onset of drought unless it is dynamically averaged over the soil profile (De Kauwe *et al*., 2016).

Uncertainties in root and stomatal responses are major drivers of TBM uncertainty in predicted *NPP* across a wide latitudinal gradient (Dietze *et al.* 2014; De Kauwe *et al.* 2013). Improved model representation of drought responses will require evaluation of underlying mechanisms as well as comparison of high level model outputs to ecosystem fluxes during drought periods. Evaluation of the response of key variables associated with alternative stomatal models against field data is needed. This is challenging as evaluation of alternative mechanisms (e.g. the hydraulic and physiological approaches) requires field level manipulation or exploitation of natural gradients and weather events coupled with substantial campaigns that include parallel measurement of many leaf parameters (e.g. ψ_{leaf}, *in situ* gas exchange and $V_{c,max}$) in coordination with plant hydraulic parameters (e.g. soil moisture content, ψ_{soil}, sap flux, hydraulic conductivity and cavitation vulnerability).

Recommendations: (10) Models should respond to soil water availability through ψ_{soil}, but variation in ψ_{soil} with soil depth needs to be incorporated (11) We need rich data sets of coordinated physiological and environmental measurements to enable evaluation of alternative modeling approaches for the representation of the response of A to drought.

Scaling physiology

543 Above, we focused primarily on leaf level responses to environmental and climate change
544 drivers, but a major challenge for model representation is how to scale process knowledge of
545 physiology and leaf level parameterization through time (seasonal change), vertically through
546 the canopy, spatially across the landscape, and also to represent photosynthetic acclimation to
547 rising temperature and C_a. These issues are discussed below.
548
549 **Effects of day length and season**
550
551 Photosynthesis responds to short-term environmental changes, but it also shows broad, regular
552 seasonal changes, especially in higher latitudes. In these regions, *A* halts in the autumn as
553 leaves senesce in deciduous species and decreases as $V_{c,max}$ is down-regulated during the cold
554 winter months in evergreens. Much of this temporal scaling of *A* is captured in TBMs through
555 phenology models and the direct temperature effects on $V_{c,max}$.
556
557 While temperature may be a major factor in driving seasonal patterns of *A*, other
558 environmental cues may be as, or even more, important. Photoperiod is known to have strong
559 effects on leaf phenology, which has indirect effects on *A*, but has not generally been
560 considered to affect *A* directly (Way & Montgomery, 2015). However, Bauerle *et al*. (2012)
561 found that photoperiod was a stronger predictor of seasonal changes in both $V_{c,max}$ and J_{max}
562 than air temperature. In that data set, $V_{c,max}$ peaked immediately after the summer solstice,
563 and declined steadily into the autumn, although air temperatures did not peak until a month or
564 more after the solstice. When this effect was accounted for with a photoperiod correction of

565 $V_{c,max}$ in CLM, the model's ability to capture seasonal patterns of atmospheric C_a was improved
566 (Bonan *et al*. 2011; Bauerle *et al*. 2012). Other papers have noted that incorporating a
567 photoperiod scalar with direct effects on $V_{c,max}$ improves estimates of seasonal carbon fluxes in
568 eddy flux studies, supporting a role for photoperiod in modulating $V_{c,max}$ (Medvigy *et al*. 2013;
569 Stoy *et al*. 2014). In controlled environments, photoperiod is tightly correlated with total leaf
570 protein content, suggesting a tradeoff between the value of protein and the cost of its
571 maintenance and provides a possible mechanistic explanation for the impact of photoperiod on
572 $V_{c,max}$ (Hannemann *et al*. 2009). However, not all PFTs show the same response to changes in
573 day length and it is possible that photoperiod corrections may be capturing leaf age effects
574 (Medlyn *et al*. 2002b; Medlyn *et al*. 2007; Busch *et al*. 2007; Lin *et al*. 2013; Stinziano *et al*.
575 2015). In the tropics, day-length is essentially constant and therefore photoperiod scalars will
576 fail to capture the well documented photosynthetic seasonality associated with tropical
577 evergreen forests (Doughty & Goulden, 2008). In dry season Amazonian evergreen forests
578 recent work has shown that a higher canopy level photosynthetic capacity associated with new
579 leaf flushing explains seasonal dynamics of photosynthetic rate (Wu *et al*. 2016a).
580 *Recommendations: (12) We need to elucidate the mechanism underlying the use of photoperiod*
581 *scalars to modify photosynthetic parameterization. (13) In order to capture photosynthetic*
582 *seasonality in tropical evergreen forests, we need to develop new approaches that are capable*
583 *of coupling prognostic leaf phenology to photosynthetic capacity.*
584
585 **Acclimation to temperature**
586

587 The short-term photosynthetic responses to temperature covered above are themselves
588 sensitive to the temperatures experienced over longer time scales (days to weeks). This longer-
589 term adjustment, known as temperature acclimation, has been widely reported and recently
590 reviewed (Smith and Dukes 2013, Way & Yamori 2014). The phenomenon is commonly
591 observed as a shift in the optimum temperature for *A* (T_{opt}), which can maximize the *A* at the
592 growth temperature (Berry & Björkman, 1980; Yamori *et al*., 2014; Kattge & Knorr, 2007). The
593 mechanistic process of acclimation and its timescale have not been well described, either
594 within or across species. At the slowest and broadest scales, the process of acclimation is
595 constrained by leaf structure and rates of leaf development and turnover. Leaves that develop
596 under one set of conditions are constrained by their existing anatomy from adjusting fully to a
597 new set of conditions (Campbell *et al*. 2007). Within a leaf, acclimation rates are driven by the
598 rates at which biochemical and physiological processes can adjust.
599
600 At the leaf scale, acclimation results from temperature-driven changes in enzyme abundances
601 and isoforms, and of membrane composition (Yamori *et al*. 2014). At low growth
602 temperatures, the abundance of Rubisco and other photosynthetic enzymes increases, and
603 some plants produce enzymes with different isoforms, which have different kinetic constants.
604 Under high growth temperatures, plants are thought to increase the stability of the thylakoid
605 membrane, and their capacity for increased electron transport. Also, some plants can produce
606 a more heat-stable form of Rubisco (Crafts-Brandner *et al*. 1997), and increase expression of
607 heat-shock proteins. Growth temperature also affects the temperature response of respiration,
608 with consequences for net *A* (e.g., Atkin & Tjoelker 2003, Way & Yamori 2014); although the

609 acclimation of respiration may affect plant growth more strongly than that of *A* for some
610 species (Way & Oren 2010), this topic lies beyond the scope of this paper and has recently been
611 considered elsewhere (Atkin *et al.* 2015).
612
613 While long-term acclimation of *A* to temperature has been observed in many species and
614 studies, fewer studies have quantified acclimation at the process level i.e. $V_{c,max}$ and J_{max}. From
615 observed responses, one may expect seasonal variation in the temperature dependence of J_{max}
616 and changes in the JV_{ratio}. Some confirmation of this was provided by Kattge & Knorr (2007)
617 who reanalysed data from 36 (primarily temperate) plants and showed that the optimum
618 temperature of $V_{c,max}$ and J_{max} increased by 0.44^{o}C and 0.33^{o}C per 1^{o}C increase of growth
619 temperature, and that the JV_{ratio} at 25^{o}C significantly decreased with increasing growth
620 temperature. However, temperature acclimation may result from different processes in
621 different species: $V_{c,max}$ and $J_{\max}$ measured at 25^{o}C were, on average, unaffected by growth
622 temperature across tree species (Way & Oren, 2010) and showed a wide variation in responses
623 across a broad range of plant growth forms (Way & Yamori 2014).
624
625 The representation of $V_{c,max}$ and $J_{\max}$ acclimation based on Kattge & Knorr (2007) has been
626 included in some models (e.g., Raddatz *et al*. 2007, Ziehn *et al*. 2011, Arneth *et al*. 2012,
627 Lombardozzi *et al*. 2015), and recent work suggests that incorporation of both photosynthetic
628 and respiratory acclimation can alter projections of land carbon storage by 10-40 Pg by the end
629 of the century (Lombardozzi *et al*. 2015, Smith *et al*. 2016). However, there is clear indication
630 that species differ in the degree to which they acclimate to temperature (e.g., Yamori *et al*.

631 2014), and no formulations have yet been developed that capture this variation across a broad
632 range of PFTs.
633
634 Researchers have recorded acclimation of different species occurring over periods lasting from
635 two days to nearly two weeks (e.g., Björkman & Badger 1979, Gunderson *et al*. 2010, Slatyer &
636 Ferrar 1977). Very limited evidence suggests that the exact timescale of acclimation may not be
637 critical for modeled estimates of GPP as long as it is in a range of approximately 3-45 days
638 (Dietze 2014) but the issue needs to be evaluated more thoroughly before that assumption is
639 widely adopted. A specific timescale does need to be specified in models to calculate growth
640 temperature, and is straightforward to identify experimentally. Kattge & Knorr (2007) assumed
641 an acclimation period of 30 days, using an average of day and night temperatures, but it is clear
642 that the bulk of biochemical and physiological adjustments happen over a shorter time period.
643 *Recommendations: (14) Physiologists need to measure thermal acclimation of the*
644 *photosynthetic traits (e.g.* $V_{c,max}$ *and* J_{max}*) that drive model outputs rather than thermal*
645 *acclimation of A. (15) We need a better understanding and model representation of thermal*
646 *acclimation across biomes, specifically the capacity and degree to which species can acclimate,*
647 *the time scales over which acclimation occurs, and the degree to which temperature acclimation*
648 *is affected by other environmental variables.*
649
650 **Acclimation to rising [CO_2]**
651

652 Photosynthetic acclimation to elevated C_a is the reduced stimulation of A that often occurs
653 following long-term growth at elevated C_a (Ainsworth & Rogers, 2007). It is the result of a
654 reduction in $V_{c,max}$ relative to J_{max} (Ainsworth & Long, 2005, Ainsworth & Rogers, 2007, Leakey
655 *et al.*, 2009, Long *et al.*, 2004, Rogers & Humphries, 2000). Notably, the reduction in
656 photosynthetic capacity typically reduces the magnitude of the stimulation of A without
657 completely eliminating it (Leakey *et al.* 2009). The acclimation response reduces allocation of N
658 to Rubisco, thereby allowing N resources to be combined with the greater C supply from
659 stimulated A at elevated C_a (Drake *et al.* 1997, Long *et al*. 2004). In fact, a meta-analysis of
660 Ainsworth & Long (2005) found that the decrease in leaf N content observed at elevated C_a was
661 largely attributable to the decrease in Rubisco. Consequently, the magnitude of any
662 photosynthetic acclimation is tightly coupled to the C and N status, and the source-sink
663 balance, of the plant (Medlyn, 1998; Ainsworth & Rogers, 2007, Ainsworth *et al.*, 2004, Leakey
664 *et al.*, 2009, Rogers *et al.*, 2009, Rogers *et al.*, 1998). For example, in severely N limited systems,
665 acclimation is strong and can be attributed to a nonspecific reduction in leaf N content (Warren
666 *et al.*, 2015), a mechanism that is currently accounted for by some TBMs in this study (Table 1).
667 Acclimation is also strong when the capacity of sinks to use photoassimilate is low, leading to
668 accumulation of leaf carbohydrates and induction of sugar signaling pathways that reduce
669 expression of Rubisco (Moore *et al.* 1999). There is evidence for variation in the acclimation
670 response among functional groups that differ in the processes limiting A at ambient C_a
671 (Ainsworth & Rogers, 2007). Acclimation is rarely observed in plants that have Rubisco-limited A
672 at current C_a and elevated C_a. As C_i rises above the inflection point on an A-C_i response curve,
673 A will become RuBP regeneration-limited, and carboxylation capacity will exceed requirements.

674 In this situation, plants grown at elevated C_a typically exhibit photosynthetic acclimation and
675 reduce their investment in Rubisco (Ainsworth & Rogers, 2007).
676
677 The TBMs in this review either do not include photosynthetic acclimation to elevated C_a or link
678 it to a non-specific reduction in leaf N content that is focused on reduced N availability and
679 constrained C:N stoichiometry (Luo *et al.*, 2004). No models currently include representation of
680 the physiological acclimation to elevated C_a described above and widely reported in Free Air
681 CO_2 Enrichment (FACE) studies (Long *et al.* 2004, Ainsworth & Rogers 2007, Leakey *et al.* 2009),
682 where the meta-analysis of Ainsworth & Long (2005) found that the decrease in leaf N content
683 observed at elevated C_a was largely attributable to the decrease in Rubisco. 2009). Recent
684 analysis has shown that failing to account for photosynthetic acclimation at elevated C_a leads to
685 an overestimation of yield in soybean (Twine *et al.*, 2013) - a legume where reductions in leaf N
686 content at elevated C_a are theoretically minimal (Rogers *et al.*, 2009). Therefore, the potential
687 for model representation of photosynthetic acclimation to elevated C_a to reduce errors of this
688 type when modeling other more N limited systems is likely substantial. In future TBMs we
689 believe it will be important to capture the mechanisms that control physiological acclimation to
690 rising C_a and not just acclimation resulting from reduced N availability. An approach that
691 reduces N allocation to Rubisco when C_a rises beyond the inflection point of PFT-specific CO_2
692 response curves would be a good first step. However, unlike thermal acclimation, no
693 algorithms have been developed to facilitate inclusion of this concept in TBMs despite the
694 substantial research from FACE experiments. Published data from FACE experiments could
695 potentially be used for development and validation of new algorithms.

Recommendation (16) We need to develop a new model representation of the physiological acclimation of photosynthesis to elevated C_a.

Leaf to canopy scaling

Due to high non-linearity of photosynthetic responses to light, temperature and *VPD*, scaling *A* from leaves to canopy remains an important challenge for models (Jarvis, 1995). Central to this challenge is TBM representation of light penetration and utilization within the canopy's vertical profile and the vertical scaling of physiology within the canopy. Analogous effects arise from within-canopy variations in temperature and *VPD*, although to a lower degree (Niinemets & Anten, 2009).

Although the average light intensity typically decreases exponentially with increasing cumulative leaf area index through the canopy, the extent of this decline is affected by the optical properties of individual leaves (including albedo) and how these change with canopy depth, season and leaf age, leaf inclination angle distribution and foliage and canopy spatial clumping (Cescatti & Niinemets, 2004; Kobayashi *et al*., 2007; Chen *et al*., 2012; Disney, 2015; Drewry *et al.* 2014; Wu *et al*. 2016a,b). Furthermore, due to gaps in the canopy, leaves at a given value of cumulative leaf area index can be sunlit or shaded, further complicating the estimation of light at the leaf surface, leaf absorption, and the subsequent numeric integration of canopy-scale photosynthetic, water, and energy fluxes (de Pury & Farquhar, 1997; Wang & Leuning, 1998; de Pury & Farquhar, 1999; Kobayashi *et al*., 2012). Here, the models differ in

718 how these scaling issues are addressed (Table 1) and based on how the canopy is considered,
719 they can be broadly divided between multi-layer models and big-leaf models.
720
721 Several TBMs have used the "big leaf" approach where a canopy approximately represents a
722 single big leaf with a single set of traits describing the photosynthetic capacity together with
723 characteristic light and temperature response functions (generally by PFT), typically scaled to
724 the canopy as a function of leaf area index (e.g., Amthor, 1994; Sands, 1996). Although
725 sometimes still used (e.g. G'DAY, Table 1), the big leaf model approach consisting of a single
726 "leaf" has been demonstrated to be prone to major integration errors due to lack of
727 consideration of sunlit and shaded leaf area classes (de Pury & Farquhar, 1997; Friend, 2001).
728 These errors were somewhat reduced by developing the "two big-leaf" model approach, which
729 consists of separate handling of a representative sunlit and a shaded big leaf (de Pury &
730 Farquhar, 1997; Chen *et al*., 1999; Dai *et al*., 2004). Indeed, separate integration of *A* for sunlit
731 and shaded leaf fractions provides a much more accurate integration of carbon and water
732 fluxes (de Pury & Farquhar, 1997; Dai *et al*., 2004), and this is the approach used in several
733 contemporary TBMs (Table 1).
734
735 Big leaf models differ in how whole-canopy $V_{c,max}$ and J_{max} values are derived (or sunlit and
736 shaded big leaf values are derived), but typically, proportionality of photosynthetic capacity and
737 average light (deemed optimal) is assumed (Table 1, Amthor, 1994; Sands, 1995a; Sands,
738 1995b). Yet, such optimality is not present in nature (Niinemets, 2012). In fact, the decline of
739 photosynthetic capacity through the canopy is much shallower than that for light (Lloyd *et al*.,

2010; Dewar *et al*. 2012; Niinemets *et al*., 2015). Such departures from optimality have been considered in some multi-layer models (Table 1), but nevertheless, only a few datasets have been used to develop global parameterizations for multi-layer models (e.g., Carswell *et al*., 2000; Lloyd *et al*., 2010). PFT and biome-dependent within-canopy acclimation patterns have recently been highlighted (Niinemets *et al*., 2015) and could be used in future model development.

Depending on the distribution of foliage inclination angles and spatial clumping, the probability for light penetration varies at a given cumulative LAI (Cescatti & Niinemets, 2004; Disney, 2015). Importantly, characteristic canopy features differ among PFTs given fundamental differences in leaf habit and growth forms (Cescatti & Niinemets, 2004), as a result of land-use, landscape legacies and past disturbance, but few TBMs take this into account. While the multi-layer models can be easily modified to incorporate different clumping and foliage inclination angles, this is much less straightforward for the big leaf models. In fact, differences in canopy architecture are part of the whole-canopy $V_{c,max}$ and J_{max} values in current big leaf models, i.e. the input values get converted to canopy-scale sunlit and shaded values blurring the definition of $V_{c,max}$ and J_{max} and making comparison with measured leaf level values impossible. Moreover, leaf optical properties and foliar traits change markedly within the vertical canopy profile (Serbin *et al*., 2014; Wu *et al*., 2016b; Yang *et al*., 2016), but are often assumed static, which will generally lead to improper representation of light interception and utilization. This improper representation will feed forward to the integration of leaf energy balance and carbon uptake. We argue that traits like $V_{c,max}$ and J_{max} should retain their original physiological

762 definition and that more effort is needed to improve the representation of canopy
763 architecture and subsequent scaling of foliar properties in TBMs. Modifications to the
764 underlying radiative transfer model (RTM) structure and scaling can help to improve the
765 representation of the canopy light environment and modeling of carbon, water, and energy
766 fluxes (Kobayashi *et al*., 2012), however increasing RTM complexity or vertical layering should
767 not come at the cost of the ability to parameterize the model. A promising means to constrain
768 these approaches is through model-data integration whereby remote sensing observations (e.g.
769 optical, LiDAR) from the leaf to landscape are used to inform the RTM structure and to
770 parameterize across spatial and temporal scales (e.g. Shiklomanov *et al*. 2016).
771 *Recommendations: (17) TBMs should not use single layer big leaf models. (18) We need better*
772 *model representation of canopy architecture and vertical scaling of foliar properties, and data to*
773 *evaluate alternative radiative transfer models and scaling approaches.*
774
775 **Canopy to landscape scaling**
776
777 There is considerable variability in plant physiological traits across space and time (Serbin *et al*.,
778 2015; Singh *et al*., 2015), even within an individual species or PFT (Kattge *et al.* 2011; Serbin *et*
779 *al*., 2014). This variability is driven by differences across vegetation types, photosynthetic
780 pathways, plant successional status, as well as a result of nutrient availability and other abiotic
781 factors. There is a propensity for strong covariance among many key physiological traits as well
782 as fundamental tradeoffs which determine the distribution of these properties across
783 landscapes. Moreover, the nonlinearity in the scaling of model processes from leaf to larger

784 regions requires careful consideration of model parameterization in order to effectively capture
785 the larger-scale emergent responses (Fisher *et al*., 2015). Parameterization with single, fixed
786 values of photosynthetic capacity likely obscures the true response of vegetation to global
787 change across landscapes, particularly at the current climatic extents of vegetation, thus
788 inadequately capturing critical plant threshold responses to factors such as temperature and
789 precipitation. The links between leaf-level observations, environmental responses and
790 emergent landscape-scale parameterizations needed for TBMs is are not straightforward, and
791 as such global parameterizations are commonly derived through the inversion of large-scale
792 datasets (e.g. Kattge *et al*., 2009; Lin *et al*., 2015). However use of such data sets can yield
793 parameterization that is inconsistent with current model structures resulting in unrealistic
794 model outputs (e.g. Bonan *et al*., 2012). Furthermore, the trade-offs among variables (e.g.
795 $V_{c,max}$ v N) are themselves scale-dependent, with slopes changing depending on whether one is
796 looking at an across-PFT evolutionary constraint, a within-PFT community response, or a within-
797 individual phenotypic response (Feng and Dietze 2014). Care must be taken to not use data
798 constraints at one scale (e.g. global) to drive responses at another scale (e.g. responses to
799 change over time).
800
801 The increasing use of trait databases (Wright *et al*., 2004; Kattge *et al*., 2011) in modeling
802 activities has started to address some of these issues by leveraging more comprehensive
803 descriptions of traits within models and across PFTs (LeBauer *et al*., 2013; Dietze *et al*., 2014;
804 Fisher *et al*., 2015). These databases should also be used to more extensively explore trait-
805 environment relationships. New, model-data integration frameworks (e.g. LeBauer *et al*., 2013;

806 Dietze *et al*., 2014) can be used to explore the capacity to adequately parameterize existing and
807 new model representations, expand PFT descriptions, as well as identify critical model
808 uncertainties and data gaps and thus prioritize observational and model development activities
809 (Dietze *et al*., 2014). Given the current diverse methods used to parameterize photosynthetic
810 parameters (Rogers, 2014), the available data (e.g. Kattge *et al*. 2011), and new opportunities
811 to markedly expand databases (e.g. Serbin *et al* 2012, De Kauwe *et al.* 2016), we recommend
812 that models should now use common parameterizations for photosynthetic parameters e.g.
813 $V_{c,max}$ and J_{max} that are constrained by the available data and consistent with known trait
814 covariance, thereby removing unnecessary uncertainty from model projections.
815
816 The capacity to utilize remote sensing observations to inform model parameterizations,
817 representations, and trait-environment relationships across spatial and temporal scales is
818 increasing (Dahlin *et al*., 2013; Serbin *et al*., 2015; Schimel *et al*., 2015; Shugart *et al*., 2015;
819 Singh *et al*., 2015). Importantly, remote sensing observations can provide a synoptic view of
820 trait variability and functional diversity across landscapes (e.g. Dahlin *et al*., 2013; Asner *et al*.
821 2015; Singh *et al*., 2015) and identify emergent relationships that could be included in next-
822 generation trait-based models. These observations can also be used as important datasets to
823 benchmark prognostic traits at the relevant spatial scales (e.g. Fisher *et al*., 2015). Proposed
824 and upcoming and satellite missions, including NASA's Hyperspectral Infrared Imager (HyspIRI)
825 mission concept (Lee *et al*., 2015) and the European Space Agencies Environmental Mapping
826 and Analysis Program (EnMAP; Guanter *et al*., 2015), will provide a critical capacity to provide
827 this information for global-scale models.

Recommendations: (19) Data constraints (e.g. trait tradeoffs) must be applied at the relevant spatial and temporal scales. (20) Where possible, TBMs should use common parameterization for photosynthetic parameters. (21) TBMs should make better use of remote sensing data to inform model parameterizations and test predictions.

Conclusion

Realistic model representation of *A*, and more broadly, plant physiological processes, should be an essential component of TBMs because that same plant physiology is determining the response of the terrestrial biosphere to global change, including the fate of the terrestrial carbon sink. However, many TBMs fail to accurately represent photosynthetic responses to key environmental variables. Here, in a subset of TBMs, we have shown marked model divergence in the representation of key physiological responses for a single well-defined PFT. We have made 21 recommendations that highlight where steps can be taken to improve existing model representation. Our recommendations include areas where immediate steps could be taken, areas where model development is hindered by a lack of physiological data and several important avenues of research that are critical to our understanding that are not currently mature enough to include in model structures. These recommendations are summarized in Fig. 6.

Current model representation of *A* has a foundation in research conducted in temperate climates. However, other biomes that are climatically sensitive and globally important are understudied, and therefore process representation in these biomes is uncertain; the Arctic and

tropics deserve particular attention. The approach taken here, i.e. evaluating how TBMs reproduce physiological responses to key environmental drivers, was found to be extremely informative by all who participated. We feel the process provides a useful template for meaningful collaboration between empiricists and modelers and that including the physiological outputs considered here as readily available diagnostic features would be a highly valuable feature to include in new TBMs. This study also highlighted the need for a multi-assumption model framework within which the modeling community and domain experts could evaluate different model structures and parameterization approaches and quantitatively evaluate their effect on model outputs. Such a framework would provide a forum where modelers and, in this case, physiologists could reach agreement over the best approaches for representing and parameterizing the sub-processes within complex TBMs.

Acknowledgements

We thank the *New Phytologist Trust* for its generous support of the 9th New Phytologist Workshop - Improving representation of photosynthesis in Earth System Models - held in Montauk, NY in April 2014. AR and SPS were supported by the Next-Generation Ecosystem Experiments (NGEE Arctic and NGEE Tropics) projects that are supported by the Office of Biological and Environmental Research in the Department of Energy, Office of Science, and through the United States Department of Energy contract No. DE-SC00112704 to Brookhaven National Laboratory; DW acknowledges support from NSERC, CFI and an Ontario ERA award. JSD received support from NSF (DEB-0955771).

872 **References**

873

874 **Ainsworth EA, Long SP. 2005.** What have we learned from 15 years of free-air CO_2 enrichment
875 (FACE)? A meta-analytic review of the responses of photosynthesis, canopy properties and
876 plant production to rising CO_2. *New Phytologist* **165**: 351-371.

877

878 **Ainsworth EA, Rogers A. 2007.** The response of photosynthesis and stomatal conductance to
879 rising CO_2: mechanisms and environmental interactions. *Plant Cell & Environment,* **30**: 258-270.

880

881 **Ainsworth EA, Rogers A, Nelson R, Long SP. 2004.** Testing the "source-sink" hypothesis of
882 down-regulation of photosynthesis in elevated CO_2 in the field with single gene substitutions in
883 Glycine max. *Agricultural and Forest Meteorology* **122**: 85-94.

884

885 **Ali AA, Xu CG, Rogers A, McDowell NG, Medlyn BE, Fisher RA, Wullschleger SD, Reich PB,**
886 **Vrugt JA, Bauerle WL, et al. 2015.** Global-scale environmental control of plant photosynthetic
887 capacity. *Ecological Applications* **25:** 2349-2365.

888

889 **Amthor JS. 1994.** Scaling CO_2-photosynthesis relationships from the leaf to the canopy.
890 *Photosynthesis Research* **39:** 321-350.

891

892 **Aphalo PJ, Jarvis PG. 1991.** Do stomata respond to relative-humidity. *Plant Cell & Environment*
893 **14**: 127-132.

894

895 **Arneth A, Mercado L, Kattge J, Booth B. 2012.** Future challenges of representing land-
896 processes in studies on land-atmosphere interactions. *Biogeosciences* **9**:3587-3599.

897

898 **Asner GP, Martin RE, Anderson CB, Knapp DE. 2015.** Quantifying forest canopy traits: Imaging
899 spectroscopy versus field survey. *Remote Sensing of Environment* **158:** 15-27.

900

901 **Atkin OK, Tjoelker MG. 2003.** Thermal acclimation and the dynamic response of plant
902 respiration to temperature. *Trends in Plant Science* **8**: 343-351.

903

904 **Atkin OK, Bloomfield KJ, Reich PB, Tjoelker MG, Asner GP, Bonal D, Bonisch G, Bradford M,**
905 **Cernusak LA, Cosio EG *et al*. 2015.** Global variability in leaf respiration in relation to climate,
906 plant functional types and leaf traits. *New Phytologist* **206:** 614-636.

907

908 **Ball TJ, Woodrow IE, Berry JA. 1987.** A model predicting stomatal conductance and its
909 contribution to the control of photosynthesis under different environmental conditions. *In* I.
910 Biggins (ed.) progress in photosynthesis research. Martinus Nijhoff Publishers, the Netherlands.
911 pp 221-224.

912

913 **Bauerle WL, Oren R, Way DA, Qian SS, Stoy PC, Thornton PE, Bowden JD, Hoffman FM,**
914 **Reynolds RF. 2012.** Photoperiodic regulation of the seasonal pattern of photosynthetic capacity

915 and the implications for carbon cycling. *Proceedings of the National Academy of Sciences of the*
916 *United States of America* **109:** 8612-8617.
917
918 **Bauerle WL, Daniels AB, Barnard DM. 2014.** Carbon and water flux responses to physiology by
919 environment interactions: a sensitivity analysis of variation in climate on photosynthetic and
920 stomatal parameters. *Climate Dynamics* **42**: 2539-2554.
921
922 **Beer C, Reichstein M, Tomelleri E, Ciais P, Jung M, Carvalhais N, Rodenbeck C, Arain MA,**
923 **Baldocchi D, Bonan GB, *et al*. 2010.** Terrestrial Gross Carbon Dioxide Uptake: Global
924 Distribution and Covariation with Climate. *Science,* **329**: 834-838.
925
926 **Bernacchi CJ, Singsaas EL, Pimentel C, Portis Jr AR, Long SP. 2001.** Improved temperature
927 response functions for models of Rubisco-limited photosynthesis. *Plant, Cell & Environment*, **24**:
928 253-259.
929
930 **Bernacchi CJ, Calfapietra C, Davey PA, Wittig VE, Scarascia-Mugnozza GE, Raines CA, Long SP.**
931 **2003.** Photosynthesis and stomatal conductance responses of poplars to free-air CO_2
932 enrichment (PopFACE) during the first growth cycle and immediately following coppice. *New*
933 *Phytologist* **159:** 609-621.
934
935 **Berry JA, Björkman O. 1980.** Photosynthetic response and adaptation to temperature in higher-
936 plants. *Annual Review of Plant Physiology and Plant Molecular Biology* **31:** 491-543.

Best MJ, Pryor M, Clark DB, Rooney GG, Essery RLH, Menard CB, Edwards JM, Hendry MA Porson A, Gedney N *et al*. 2011. The Joint UK Land Environment Simulator (JULES), model description – Part 1: Energy and water fluxes. *Geoscientific Model Development* **4:** 677-699.

Bjorkman O, Badger M. 1979. Time course of thermal acclimation of the photosynthetic apparatus in Nerium oleander. *Carnegie Inst. Washington Yearb.* **78:** 262-75

Boden TA, Marland G, Andres RJ. 2013. Global, regional and national fossil-fuel CO_2 emissions., Oak Ridge, Carbon Dioxide Information Analysis Center, Oak Ridge National Laboratory, U.S. Department of Energy.

Bonan GB, Lawrence PJ, Oleson KW, Levis S, Jung M, Reichstein M, Lawrence DM, Swenson SC. 2011. Improving canopy processes in the Community Land Model version 4 (CLM4) using global flux fields empirically inferred from FLUXNET data. *Journal of Geophysical Research* **116:** G02014

Bonan GB, Oleson KW, Fisher RA, Lasslop G, Reichstein M. 2012. Reconciling leaf physiological traits and canopy flux data: Use of the TRY and FLUXNET databases in the Community Land Model version 4. *Journal of Geophysical Research-Biogeosciences* **117**, G02026

Bonan GB, Williams M, Fisher RA, Oleson KW. 2014. Modeling stomatal conductance in the earth system: linking leaf water-use efficiency and water transport along the soil-plant-atmosphere continuum. *Geoscientific Model Development* **7**, 2193-2222.

Bunce JA. 2000. Responses of stomatal conductance to light, humidity and temperature in winter wheat and barley grown at three concentrations of carbon dioxide in the field. *Global Change Biology* **6:** 371-382

Busch F. 2013. Current methods for estimating the rate of photorespiration in leaves. *Plant Biology* **15:** 648-655.

Busch F, Hüner NPA, Ensminger I. 2007. Increased air temperature during simulated autumn conditions does not increase photosynthetic carbon gain but affects the dissipation of excess energy in seedlings of the evergreen conifer Jack pine. *Plant Physiology* **143:** 1242-1251.

Campbell C, Atkinson L, Zaragoza-Castells J, Lundmark M, Atkin O, Hurry V. 2007. Acclimation of photosynthesis and respiration is asynchronous in response to changes in temperature regardless of plant functional type. *New Phytologist* **176:** 375–389.

Carswell FE, Meir P, Wandelli EV, Bonates LCM, Kruijt B, Barbosa EM, Nobre AD, Grace J, Jarvis PG. 2000. Photosynthetic capacity in a central Amazonian rain forest. *Tree Physiology* **20:** 179-186.

Cescatti A, Niinemets Ü 2004. Sunlight capture. Leaf to landscape. In: Smith WK, Vogelmann TC, Chritchley C eds. Photosynthetic adaptation. Chloroplast to landscape. Berlin: Springer Verlag, 42-85.

Chaves MM, Flexas J, Pinheiro C. 2009. Photosynthesis under drought and salt stress: regulation mechanisms from whole plant to cell. *Annals of Botany*, **103:** 551-560.

Chen JM, Liu J, Cihlar J, Goulden ML. 1999. Daily Canopy Photosynthesis Model Through Temporal and Spatial Scaling for Remote Sensing Applications. *Ecological Modelling* **124:** 99-119.

Chen JM, Mo G, Pisek J, Liu J, Deng F, Ishizawa M, Chan D. 2012. Effects of foliage clumping on the estimation of global terrestrial gross primary productivity. *Global Biogeochemical Cycles* **26**, GB1019.

Christmann A, Weiler EW, Steudle E, Grill E. 2007. A hydraulic signal in root-to-shoot signalling of water shortage. *Plant Journal* **52:** 167-174.

Ciais P, Gasser T, Paris JD, Caldeira K, Raupach MR, Canadell JG, Patwardhan A, Friedlingstein P, Piao SL *et al*. 2013. Attributing the increase in atmospheric CO_2 to emitters and absorbers. *Nature Climate Change* **3:** 926-930.

Collatz GJ, Ball JT, Grivet C, Berry JA (1991) Physiological and environmental regulation of stomatal conductance, photosynthesis and transpiration – a model that includes laminar boundary layer. *Agricultural and Forest Meteorology* **54:** 107-136.

Clark DB, Mercado LM, Sitch S, Jones CD, Gedney N, Best MJ, Pryor M, Rooney GG, Essery RLH, Blyth E *et al*. 2011. The Joint UK Land Environment Simulator (JULES), model description – Part 2: Carbon fluxes and vegetation dynamics. *Geoscientific Model Development* **4:** 701-722.

Cowan IR, Farquhar GD. 1977. Stomatal function in relation to leaf metabolism and environment. In: Integration of Activity in the Higher Plant (ed. Jennings DH), pp. 471–505. Cambridge University Press, Cambridge.

Crafts-Brandner SJ, van de Loo FJ, Salvucci ME. 1997. The two forms of ribulose-1,5-bisphosphate carboxylase/oxygenase activase differ in sensitivity to elevated temperature. *Plant Physiology*, 114, 439-444.

Cramer W, Bondeau A, Woodward FI, Prentice IC, Betts RA, Brovkin V, Cox PM, Fisher V, Foley JA, Friend AD *et al*. 2001. Global response of terrestrial ecosystem structure and function to CO_2 and climate change: results from six dynamic global vegetation models. *Global Change Biology* **7**: 357-373.

1024 **Dai Y-J, Dickinson RE, Wang YP. 2004.** A two-big-leaf model for canopy temperature,
1025 photosynthesis, and stomatal conductance. *Journal of Climate* **17:** 2281-2299.
1026
1027 **Dahlin KM, Asner GP, Field CB. 2013.** Environmental and community controls on plant canopy
1028 chemistry in a Mediterranean-type ecosystem. *Proceedings of the National Academy of*
1029 *Sciences* **110:** 6895-6900.
1030
1031 **Drewry DT, Kumar P, Long SP. 2014.** Simultaneous improvement in productivity, water use, and
1032 albedo through crop structural modification. *Global Change Biology* **20**: 1955-1967.
1033
1034 **de Pury DGG, Farquhar GD. 1997.** Simple scaling of photosynthesis from leaves to canopies
1035 without the errors of big-leaf models. *Plant, Cell & Environment* **20:** 537-557.
1036
1037 **de Pury DGG, Farquhar GD. 1999.** A commentary on the use of a sun/shade model to scale
1038 from the leaf to a canopy. *Agricultural and Forest Meteorology* **95:** 257-260.
1039
1040 **De Beeck MO, Gielen B, Jonckheere I, Samson R, Janssens IA, Ceulemans R. 2010.** Needle age-
1041 related and seasonal photosynthetic capacity variation is negligible for modelling yearly gas
1042 exchange of a sparse temperate Scots pine forest. *Biogeosciences,* **7**: 199-215.
1043
1044 **De Kauwe MG, Medlyn BE, Zaehle S Walker AP, Dietze MC, Hickler T, Jain AK, Luo YQ, Parton**
1045 **WJ, Prentice IC. 2013.** Forest water use and water use efficiency at elevated CO2: a model-data

intercomparison at two contrasting temperate forest FACE sites. *Global Change Biology* **19**, 1759-1779.

De Kauwe MG, Zhou SX, Medlyn BE, Pitman AJ, Wang YP, Duursma RA, Prentice IC. 2015. Do land surface models need to include differential plant species responses to drought? Examining model predictions across a mesic-xeric gradient in Europe. *Biogeosciences* **12**, 7503-7518.

De Kauwe MG, Lin YS, Wright IJ, Medlyn BE, Crous KY, Ellsworth DS, Maire V, Prentice IC, Atkin OK, Rogers A *et al*. 2016. A test of the 'one-point method' for estimating maximum carboxylation capacity from field-measured, light-saturated photosynthesis. *New Phytologist* **210:** 1130-1144.

Dewar RC. 2002. The Ball-Berry-Leuning and Tardieu-Davies stomatal models: synthesis and extension within a spatially aggregated picture of guard cell function. *Plant Cell & Environment* **25:** 1383-1398.

Dewar RC, Tarvainen L, Parker K, Wallin G, Mcmurtrie RE. 2012. Why does leaf nitrogen decline within tree canopies less rapidly than light? An explanation from optimization subject to a lower bound on leaf mass per area. *Tree Physiology* **32**, 520-534.

Dietze MC. 2014. Gaps in knowledge and data driving uncertainty in models of photosynthesis. *Photosynthesis Research* **119**: 3-14.

Disney M. 2015. Remote sensing of vegetation: potentials, limitations, developments and applications. In: Hikosaka K, Anten NPR, Niinemets Ü eds. Canopy photosynthesis: from basics to applications. Berlin: Springer Verlag, pp289-331.

Doughty CE, Goulden ML. 2008. Seasonal patterns of tropical forest leaf area index and CO_2 exchange. *Journal of Geophysical Research: Biogeosciences* **113:** G00B07

Egea G, Verhoef A, Vidale PL. 2011. Towards an improved and more flexible representation of water stress in coupled photosynthesis-stomatal conductance models. *Agricultural and Forest Meteorology* **151**: 1370-1384.

Ethier GJ, Livingston NJ. 2004. On the need to incorporate sensitivity to CO_2 transfer conductance into the Farquhar-von Caemmerer-Berry leaf photosynthesis model. *Plant, Cell & Environment* **27:** 137-153.

Farquhar GD, von Caemmerer S. Berry JA. 1980. A biochemical-model of photosynthetic CO_2 assimilation in leaves of C_3 species. *Planta* **149**: 78-90.

Feng X, Dietze M. 2013. Scale dependence in the effects of leaf ecophysiological traits on photosynthesis: Bayesian parameterization of photosynthesis models. *New Phytologist* **200:** 1132-1144.

Fisher JB, Badgley G, Blyth E. 2012. Global nutrient limitation in terrestrial vegetation. *Global Biogeochemical Cycles* **26:** GB3007.

Fisher JB, Huntzinger DN, Schwalm CR, Sitch S. 2014. Modeling the Terrestrial Biosphere. *Annual Review of Environment and Resources* **39:** 91-123.

Fisher RA, Muszala S, Verteinstein M, Lawrence P, Xu C, McDowell NG, Knox RG, Koven CD, Holm J, Rogers BM *et al*. 2015. Taking off the training wheels: the properties of a dynamic vegetation model without climate envelopes, CLM4.5(ED). *Geoscientific Model Development* **8:** 3593-3619.

Flexas J, Barbour MM, Brendel O, Cabrera HM, Carriqui M, Diaz-Espejo A, Douthe C, Dreyer E, Ferrio JP, Gago J, *et al*. 2012. Mesophyll diffusion conductance to CO_2: An unappreciated central player in photosynthesis. *Plant Science* **193**: 70-84.

Foley JA, Prentice IC, Ramankutty N, Levis S, Pollard D, Sitch S, Haxeltine A. 1996. An integrated biosphere model of land surface processes, terrestrial carbon balance, and vegetation dynamics. *Global Biogeochemical Cycles* **10:** 603-628.

Friend AD. 2010. Terrestrial plant production and climate change. *Journal of Experimental Botany* **61:** 1293-1309.

Friedlingstein P, Cox P, Betts R, Bopp L, von Bloh W, Brovkin V, Cadule P, Doney S Eby M, Fung I *et al.* 2006. Climate-carbon cycle feedback analysis: Results from the (CMIP)-M-4 model intercomparison. *Journal of Climate* **19**: 3337-3353.

Friedlingstein P, Meinshausen M, Arora VK, Jones CD, Anav A, Liddicoat SK, Knutti R. 2014. Uncertainties in CMIP5 Climate Projections due to Carbon Cycle Feedbacks. *Journal of Climate* **27:** 511-526.

Friend AD. 2001. Modelling canopy CO2 fluxes: are 'big-leaf' simplifications justified? *Global Ecology and Biogeography* **10:** 603-619.

Galmés J, Kapralov MV, Copolovici LO, Hermida-Carrera C, Niinemets Ü. 2015. Temperature responses of the Rubisco maximum carboxylase activity across domains of life: phylogenetic signals, trade-offs, and importance for carbon gain. *Photosynthesis Research* **123**: 183-201.

Gregory JM, Jones CD, Cadule P, Friedlingstein P. 2009. Quantifying Carbon Cycle Feedbacks. *Journal of Climate* **22**: 5232-5250.

Gu LH, Baldocchi D, Verma SB, Black TA, Vesala T, Falge EM, Dowty PR. 2002. Advantages of diffuse radiation for terrestrial ecosystem productivity. *Journal of Geophysical Research-Atmospheres* **107**: 4050.

Guanter L, Kaufmann H, Segl K, Foerster S, Rogass C, Chabrillat S, Kuester T, Hollstein A, Rossner G, Chlebek C, *et al*. 2015. The EnMAP Spaceborne Imaging Spectroscopy Mission for Earth Observation. *Remote Sensing* **7:** 8830.

Gunderson CA, O'Hara KH, Campion CM, Walker AV, Edwards NT. 2010. Thermal plasticity of photosynthesis: the role of acclimation in forest responses to a warming climate. *Global Change Biology* **16:** 2272-2286.

Hannemann J, Poorter H, Usadel B, Blasing OE, Finck A, Tardieu F, Atkin OK, Pons T, Stitt M, Gibon Y. 2009. Xeml Lab: a tool that supports the design of experiments at a graphical interface and generates computer-readable metadata files, which capture information about genotypes, growth conditions, environmental perturbations and sampling strategy. *Plant Cell & Environment* **32**: 1185-1200.

Hari P, Makela A, Korpilahti E, Holmberg M. 1986. Optimal control of gas exchange. *Tree Physiology* **2**: 169-175.

Harper A, Cox P, Friedlingstein P, Wiltshire A, Jones C, Sitch S, Mercado LM, Roberston E, Kattge J, *et al*. 2016. Improved representation of plant functional types and physiology in the Joint UK Land Environment Simulator (JULES v4.2) using plant trait information. *Geoscientific Model Development*. doi:10.5194/gmd-2016-22.

Huntingford C, Smith DM, Davies WJ, Falk R, Sitch S, Mercado LM. 2015. Combining the [ABA] and net photosynthesis-based model equations of stomatal conductance. *Ecological modelling* **300:** 81–88.

IPCC. 2013. Climate Change 2013: The Physical Science Basis. Contribution of Working Group I to the Fifth Assessment Report of the Intergovernmental Panel on Climate Change. (eds Stocker TF, Qin D, Plattner G-K, Tignor M, Allen SK, Boschung J, Nauels A, Xia Y, Bex V, Midgley PM) pp 1535, Cambridge University Press, Cambridge, United Kingdom and New York, NY, USA.

Jacobs CMJ. 1994. Direct impact of atmospheric CO_2 enrichment on regional transpiration. PhD thesis, Wageningen Agricultural University, Wageningen, the Netherlands, ISBN 90-5485-250-X,

Jarvis PG. 1995. Scaling processes and problems. *Plant, Cell & Environment* **18:** 1079-1089.

Jones AM. 2016. A new look at stress: abscisic acid patterns and dynamics at high-resolution. Tansley insight. *New Phytologist* **210:** 38-44

Jordan DB, Ogren WL. 1984. The CO_2/O_2 specificity of ribulose 1,5-bisphosphate carboxylase/oxygenase. Dependence on ribulose bisphosphate concentration, pH and temperature. *Planta* **161**: 308-313.

June T, Evans JR, Farquhar GD. 2004. A simple new equation for the reversible temperature dependence of photosynthetic electron transport: a study on soybean leaf. *Functional Plant Biology* **31:** 275-283

Kattge J, Knorr W. 2007. Temperature acclimation in a biochemical model of photosynthesis: a reanalysis of data from 36 species. *Plant Cell and Environment* **30**: 1176-1190.

Kattge J, Knorr W, Raddatz TJ, Wirth C. 2009. Quantifying photosynthetic capacity and its relationship to leaf nitrogen content for global-scale terrestrial biosphere models. *Global Change Biology* **15:** 976-991.

Kattge J, Diaz S, Lavorel S *et al.* 2011. TRY - a global database of plant traits. *Global Change Biology,* **17**, 2905-2935.

Katul G, Manzoni S, Palmroth S, Oren R. 2010. A stomatal optimization theory to describe the effects of atmospheric CO2 on leaf photosynthesis and transpiration. *Annals of Botany* **105**, 431-442.

Keenan T, Sabate S, Gracia C. 2010. The importance of mesophyll conductance in regulating forest ecosystem productivity during drought periods. *Global Change Biology* **16**: 1019-1034.

Kelly JWG, Duursma RA, Atwell BA, Tissue DT, Medlyn BE. 2015. Drought x CO_2 interactions in trees: a test of the low-C_i mechanism. *New Phytologist* **209:** 1600-1612

Knorr W, Heimann M. 2001. Uncertainties in global terrestrial biosphere modeling 1. A comprehensive sensitivity analysis with a new photosynthesis and energy balance scheme. *Global Biogeochemical Cycles* **15:** 207-225.

Kobayashi H, Suzuki R, Kobayashi S. 2007. Reflectance seasonality and its relation to the canopy leaf area index in an eastern Siberian larch forest: Multi-satellite data and radiative transfer analyses. *Remote Sensing of Environment* **106**: 238-252.

Kobayashi H, Baldocchi DD, Ryu Y, Chen Q, Ma S, Osuna JL, Ustin SL. 2012. Modeling energy and carbon fluxes in a heterogeneous oak woodland: A three-dimensional approach. *Agricultural and Forest Meteorology* **152**: 83-100.

Kull O, Kruijt B. 1998. Leaf photosynthetic light response: a mechanistic model for scaling photosynthesis to leaves and canopies. *Functional Ecology* **12**: 767-777.

Leakey ADB, Ainsworth EA, Bernacchi CJ, Rogers A, Long SP, Ort DR. 2009. Elevated CO_2 effects on plant carbon, nitrogen, and water relations: six important lessons from FACE. *Journal of Experimental Botany* **60**: 2859-2876.

Lebauer DS, Wang D, Richter KT, Davidson CC, Dietze MC. 2013. Facilitating feedbacks between field measurements and ecosystem models. *Ecological Monographs* **83:** 133-154.

Lee CM, Cable ML, Hook SJ, Green RO, Ustin SL, Mandl DJ, Middleton EM. 2015. An introduction to the NASA Hyperspectral InfraRed Imager (HyspIRI) mission and preparatory activities. *Remote Sensing of Environment* **167:** 6-19.

Le Quéré C, Moriarty R, Andrew R *et al.* 2015. Global Carbon Budget 2015. *Earth System Science Data Discussions,* **7**: 349-396.

Leuning R. 1995. A critical appraisal of a combined stomatal-photosynthesis model for C3 plants. *Plant Cell & Environment*, **18:** 339-355.

Leuning R, Tuzet A, Perrier A. 2004. Stomata as part of the soil-plant-atmosphere continuum. In: Forests at the Land-Atmosphere Interface (eds M. Mencuccini, J. Grace, J. Moncrieff and K.G. McNaughton) CAB International, Oxford. pp 9 - 28.

Lin YS, Medlyn BE, Ellsworth DS. 2012. Temperature responses of leaf net photosynthesis: the role of component processes. *Tree Physiology* **32:** 219-231

Lin YS, Medlyn BE, DeKauwe MG, Ellsworth DS. 2013. Biochemical photosynthetic responses to temperature: how do interspecific differences compare with seasonal shifts? *Tree Physiology* **33:** 793-806

Lin YS, Medlyn BE, Duursma RA Prentice IC, Wang H, Baig S, Eamus D, Resco de Dios V, Mitchell P Ellsworth DS *et al.* 2015. Optimal stomatal behaviour around the world. *Nature Climate Change* **5:** 459-464.

Lloyd J, Patiño S, Paiva RQ, Nardoto GB, Quesada CA, Santos AJB, Baker TR, Brand WA, Hilke I, Gielmann H, *et al*. 2010. Optimisation of photosynthetic carbon gain and within-canopy gradients of associated foliar traits for Amazon forest trees. *Biogeosciences* **7:** 1833-1859.

Lobell DB, Roberts MJ, Schlenker W, Braun N, Little BB, Rejesus RM, Hammer GL. 2014. Greater Sensitivity to Drought Accompanies Maize Yield Increase in the US Midwest. *Science* **344**, 516-519.

Lombardozzi D, Bonan G, Smith NG, Dukes JS, Fisher R. 2015. Temperature acclimation of photosynthesis and respiration: a key uncertainty in the carbon cycle-climate feedback. *Geophysical Research Letters* **42**: 8624-8631.

Long SP. 1991. Modification of the response of photosynthetic productivity to rising temperature by atmospheric CO_2 concentration - has its importance been underestimated. *Plant Cell & Environment* **14**, 729-739.

Long SP, Drake B. 1991. Effect of the long-term elevation of CO_2 concentration in the field on the quantum yield of photosynthesis of the C3 sedge, *Scirpus olneyi*. *Plant Physiology* **96**: 221-226.

Long SP, Postl WF, Bolhar-Nordenkampf HR. 1993. Quantum yields for uptake of carbon dioxide in C3 vascular plants of contrasting habitats and taxonomic groupings. *Planta* **189:** 226-234.

Long SP, Ainsworth EA, Rogers A, Ort DR. 2004. Rising atmospheric carbon dioxide: plants face the future. *Annual Review of Plant Biology* **55:** 591-628.

Lu ZM, Quinones MA, Zeiger E. 2000. Temperature dependence of guard cell respiration and stomatal conductance co-segregate in an F_2 population of Pima cotton. *Australian Journal of Plant Physiology* **27:** 457-462

Luo Y, Su B, Currie WS, Dukes JS, Finzi AF, Hartwig U, Hungate B, McMurtrie RE, Oren R, Parton WJ *et al.* 2004. Progressive nitrogen limitation of ecosystem responses to rising atmospheric carbon dioxide. *Bioscience* **54:** 731-739.

Medlyn BE, Berbigier P, Clement R, Grelle A, Loustau D, Linder S, Wingate L, Jarvis PG, Sigurdsson BD, McMurtrie RE. 2005. Carbon balance of coniferous forests growing in contrasting climates: Model-based analysis. *Agricultural and Forest Meteorology* **131:** 97-124.

Medlyn BE, Dreyer E, Ellsworth DS, Forstreuter M, Harley PC, Kirschbaum MUF, Le Roux X, Montpied P, Strassemeyer J, Walcroft A, *et al*. 2002a. Temperature response of parameters of a biochemically based model of photosynthesis. II. A review of experimental data. *Plant, Cell & Environment* **25**: 1167-1179.

Medlyn BE, Loustau D, Delzon S. 2002b. Temperature response of parameters of a biochemically based model of photosynthesis. I. Seasonal changes in mature maritime pine (Pinus pinaster Ait.). *Plant, Cell & Environment* **25:** 1155-1165

Medlyn BE, Pepper DA, O'Grady AP, Keith H. 2007. Linking leaf and tree water use with an individual-tree model. *Tree Physiology* **27**: 1687-1699

1299 **Medlyn BE, Duursma RA, Eamus D, Ellsworth DS, Prentice IC, Barton CVM, Crous KY, De**
1300 **Angelis P, Freeman M, Wingate L. 2011.** Reconciling the optimal and empirical approaches to
1301 modelling stomatal conductance. *Global Change Biology,* **17**, 2134-2144.
1302
1303 **Medlyn BE, De Kauwe MG, Zaehle S, Walker AP, Duursma RA, Luus K, Mishurov M, Pak B,**
1304 **Smith B, Wang YPP, *et al*. 2016.** Using models to guide field experiments: *a priori* predictions
1305 for the CO_2 response of a nutrient- and water- limited native Eucalypt woodland. *Global*
1306 *Change Biology* **8:** 2834-2851.
1307
1308 **Medvigy D, Wofsy SC, Munger JW, Hollinger DY, Moorcroft PR. 2009.** Mechanistic scaling of
1309 ecosystem function and dynamics in space and time: Ecosystem Demography model version 2.
1310 *Journal of Geophysical Research-Biogeosciences* **114**. GO1002.
1311
1312 **Medvigy D. Jeong S-J, Clark KL, Skowronski NS, Schäfer KVR. 2013.** Effects of seasonal variation
1313 of photosynthetic capacity on the carbon fluxes of a temperate deciduous forest. *Journal of*
1314 *Geophysical Research* **118:** 1703-1714.
1315
1316 **Meir P, Mencuccini M, Dewar RC. 2015.** Drought-related tree mortality: addressing the gaps in
1317 understanding and prediction. *New Phytologist* **207:** 28-33.
1318
1319 **Mercado LM, Bellouin N, Sitch S, Boucher O, Huntingford C, Wild M, Cox, PM. 2009.** Impact of
1320 changes in diffuse radiation on the global land carbon sink. *Nature* **458:** 1014-1017.

Moorcroft PR, Hurtt GC, Pacala SW. 2001. A method for scaling vegetation dynamics: The ecosystem demography model (ED). *Ecological Monographs* **71:** 557-585.

Mott KA. 2009. Opinion: Stomatal responses to light and CO_2 depend on the mesophyll. *Plant Cell & Environment* **32:** 1479-1486.

Niinemets U, Diaz-Espejo A, Flexas J, Galmes J. Warren CR. 2009. Importance of mesophyll diffusion conductance in estimation of plant photosynthesis in the field. *Journal of Experimental Botany* **60**: 2271-2282.

Niinemets U, Keenan T. 2014. Photosynthetic responses to stress in Mediterranean evergreens: Mechanisms and models. *Environmental and Experimental Botany* **103**: 24-41.

Niinemets U, Tenhunen JD, Beyschlag W. 2004. Spatial and age-dependent modifications of photosynthetic capacity in four Mediterranean oak species. *Functional Plant Biology* **31**: 1179-1193.

Niinemets Ü. 2012. Optimization of foliage photosynthetic capacity in tree canopies: towards identifying missing constraints. *Tree Physiology* **32:** 505-509.

Niinemets Ü, Anten NPR 2009. Packing the photosynthesis machinery: from leaf to canopy. In: Laisk A, Nedbal L, Govindjee eds. Photosynthesis in silico: understanding complexity from molecules to ecosystems. Berlin: Springer Verlag, 363-399.

Niinemets Ü, Keenan TF, Hallik L. 2015. Tansley review. A worldwide analysis of within-canopy variations in leaf structural, chemical and physiological traits across plant functional types. *New Phytologist* **205:** 973-993.

Oleson KW, Lawrence DM, Bonan GB, Drewniak B, Huang M, Koven CD, Levis S, Li F, Riley WJ, Subin ZM *et al*. 2013. Technical description of version 4.5 of the Community Land Model (CLM). NCAR Technical Note NCAR/TN-503+STR. National Center for Atmospheric Research, Boulder, Colorado. 420 pp.

Orr DJ, Alcântara A, Kapralov MV, Andralojc PJ, Carmo-Silva E, Parry MAJ. 2016. Surveying Rubisco diversity and temperature response to improve crop photosynthetic efficiency. *Plant Physiology*. doi:10.1104/00.16.00750. In Press.

Ort DR, Long SP. 2014. Limits on yields in the corn belt. *Science* **344**: 483-484.

Raddatz T, Reick CH, Knorr W, Kattge J, Roeckner E, Schnur R, Schnitzler K-G, Wetzel P, Jungclaus J. 2007. Will the tropical land biosphere dominate the climate–carbon cycle feedback during the twenty-first century? *Climate Dynamics* **29:** 565–574.

Reich PB. 2014. The world-wide 'fast-slow' plant economics spectrum: a traits manifesto. *Journal of Ecology* **102:** 275-301.

Rogers A. 2014. The use and misuse of $V_{c,max}$ in Earth System Models. *Photosynthesis Research* **119**: 15-29.

Rogers A, Ainsworth EA, Leakey ADB. 2009. Will elevated carbon dioxide concentration amplify the benefits of nitrogen fixation in legumes? *Plant Physiology* **151**: 1009-1016.

Rogers A, Fischer BU, Bryant J, Frehner M, Blum H, Raines CA, Long SP. 1998. Acclimation of photosynthesis to elevated CO_2 under low-nitrogen nutrition is affected by the capacity for assimilate utilization. Perennial ryegrass under free-air CO_2 enrichment. *Plant Physiology* **118**: 683-689.

Rogers A, Humphries SW. 2000. A mechanistic evaluation of photosynthetic acclimation at elevated CO_2. *Global Change Biology* **6**: 1005-1011.

Salvucci ME, Crafts-Brandner SJ. 2004a. Inhibition of photosynthesis by heat stress: the activation state of Rubisco as a limiting factor in photosynthesis. *Physiologia Plantarum* **120**: 179-186.

Salvucci ME, Crafts-Brandner SJ. 2004b. Relationship between the heat tolerance of photosynthesis and the thermal stability of rubisco activase in plants from contrasting thermal environments. *Plant Physiology* **134**: 1460-1470.

Sage RF, Sharkey TD. 1987. The effect of temperature on the occurance of O_2 and CO_2 insensitive photosynthesis in field-grown plants. *Plant Physiology* **84**: 658-664.

Sage RF, Kubien DS. 2007. The temperature response of C_3 and C_4 photosynthesis. *Plant Cell & Environment* **30:** 1086-1106

Sands PJ. 1995a. Modelling canopy production. I. Optimal distribution of photosynthetic resources. *Australian Journal of Plant Physiology* **22:** 593-601.

Sands PJ. 1995b. Modelling canopy production. II. From single-leaf photosynthetic parameters to daily canopy photosynthesis. *Australian Journal of Plant Physiology* **22:** 603-614.

Sands PJ. 1996. Modelling canopy production. III. Canopy light-utilisation efficiency and its sensitivity to physiological and environmental variables. *Australian Journal of Plant Physiology* **23:** 103-114.

Sato H, Kumagai TO, Takahashi A, Katul GG. 2015. Effects of different representations of stomatal conductance response to humidity across the African continent under warmer CO2-enriched climate conditions. *Journal of Geophysical Research-Biogeosciences* **120**: 979-988.

Sauter A, Davies WJ, Hartung W. 2001. The long-distance abscisic acid signal in the droughted plant: the fate of the hormone on its way from root to shoot. *Journal of Experimental Botany* **52:** 1991–1997.

Scafaro AP, Yamori W, Carmo-Silva AE, Salvucci ME, Von Caemmerer S, Atwell BJ. 2012. Rubisco activity is associated with photosynthetic thermotolerance in a wild rice (*Oryza meridionalis*). *Physiologia Plantarum* **146:** 99-109.

Scheiter S, Langan L, Higgins SI. 2013. Next-generation dynamic global vegetation models: learning from community ecology. *New Phytologist* **198:** 957-969.

Serbin SP, Dillaway DN, Kruger EL, Townsend PA. 2012. Leaf optical properties reflect variation in photosynthetic metabolism and its sensitivity to temperature. *Journal of Experimental Botany* **63**: 489-502.

Serbin SP, Singh A, McNeil BE, Kingdon CC, Townsend PA. 2014. Spectroscopic determination of leaf morphological and biochemical traits for northern temperate and boreal tree species. *Ecological Applications* **24:** 1651-1669.

Sharkey TD. 1985. Photosynthesis in intact leaves of C-3 plants - physics, physiology and rate limitations. *Botanical Review* **51**: 53-105.

Shiklomanov AN, Dietze MC, Viskari T, Townsend PA, Serbin SP. 2016. Quantifying the influences of spectral resolution on uncertainty in leaf trait estimates through a Bayesian approach to RTM inversion. *Remote Sensing of Environment* **183:** 226-238.

Singh A, Serbin SP, McNeil BE, Kingdon CC, Townsend PA. 2015. Imaging spectroscopy algorithms for mapping canopy foliar chemical and morphological traits and their uncertainties. *Ecological Applications* **25:** 2180-2197

Shugart HH, Asner GP, Fischer R, Huth A, Knapp N, Le Toan T, Shuman JK. 2015. Computer and remote-sensing infrastructure to enhance large-scale testing of individual-based forest models. *Frontiers in Ecology and the Environment* **13:** 503-511.

Singsaas EL, Ort DR, Delucia EH. 2001. Variation in measured values of photosynthetic quantum yield in ecophysiological studies. *Oecologia* **128:** 15-23.

Slatyer RO, Ferrar PJ. 1977. Altitudinal variation in the photosynthetic characteristics of snow gum, *Eucalyptus paucijlora* Sieb. Ex. Spreng. V. Rate of acclimation to an altered growth environment. *Australian Journal of Plant Physiology* **4:** 595-609

Slot M, Garcia MN, Winter K. 2016. Temperature response of CO_2 exchange in three tropical tree species. *Functional Plant Biology*, **43:** 468-478.

Smith NG, Dukes JS. 2013. Plant respiration and photosynthesis in global-scale models: incorporating acclimation to temperature and CO_2. *Global Change Biology* **19**:45-63.

Smith NG, Malyshev SL, Shevliakova E, Kattge J, Dukes JS. 2016. Foliar temperature acclimation reduces simulated carbon sensitivity to climate. *Nature Climate Change* **6:** 407

Stinziano J, Hüner NPA, Way DA. 2015. Warming delays autumn declines in photosynthetic capacity in a boreal conifer, Norway spruce (*Picea abies*). *Tree Physiology* **35:** 1303-1313.

Stoy PC, Trowbridge AM, Bauerle WL. 2014. Controls on seasonal patterns of maximum ecosystem carbon uptake and canopy-scale photosynthetic light response: contributions from both temperature and photoperiod. *Photosynthesis Research* **119:** 49-64.

Suits NS, Denning AS, Berry JA, Still CJ, Kaduk J, Miller JB, Baker IT. 2005. Simulation of carbon isotope discrimination of the terrestrial biosphere. *Global Biogeochemical Cycles* **19:** B1017.

Sun Y, Gu LH, Dickinson RE, Pallardy SG, Baker J, Cao YH, DaMatta FM, Dong XJ, Ellsworth DS, Van Goethem D. 2014. Asymmetrical effects of mesophyll conductance on fundamental

photosynthetic parameters and their relationships estimated from leaf gas exchange measurements. *Plant Cell & Environment* **37**: 978-994.

Tardieu F, Davies WJ. 1993. Integration of hydraulic and chemical signaling in the control of stomatal conductance and water status of droughted plants. *Plant Cell & Environment* **16:** 341-349.

Teskey R, Wertin T, Bauweraerts I, Ameye M, Mcguire MA, Steppe K. 2015. Responses of tree species to heat waves and extreme heat events. *Plant Cell & Environment* **38**: 1699-1712.

Tholen D, Ethier G, Genty B, Pepin S, Zhu XG. 2012. Variable mesophyll conductance revisited: theoretical background and experimental implications. *Plant Cell & Environment* **35**: 2087-2103.

Thum T, Aalto T, Laurila T, Aurela M, Kolari P, Hari P. 2007. Parametrization of two photosynthesis models at the canopy scale in a northern boreal Scots pine forest. *Tellus Series B-Chemical and Physical Meteorology* **59:** 874-890.

Tuzet A, Perrier A, Leuning R. 2003. A coupled model of stomatal conductance, photosynthesis and transpiration. *Plant Cell & Environment* **26**: 1097-1116.

Twine TE, Bryant JJ, Richter K, Bernacchi CJ, Mcconnaughay KD, Morris SJ, Leakey ADB. 2013. Impacts of elevated CO_2 concentration on the productivity and surface energy budget of the soybean and maize agroecosystem in the Midwest USA. *Global Change Biology* **19**: 2838-2852.

van Bodegom PM, Douma JC, Verheijen LM. 2014. A fully traits-based approach to modeling global vegetation distribution. *Proceedings of the National Academy of Sciences of the United States of America* **111**: 13733-13738.

von Caemmerer S. 2000. *Biochemical models of leaf photosynthesis* (vol. 2). CSIRO Publishing, Collingwood, Australia.

von Caemmerer S, Evans JR. 1991. Determination of the average partial pressure of CO_2 in chloroplast from leaves of several C_3 plants. *Australian Journal Plant Physiology* **18**: 287-305.

von Caemmerer S, Evans JR. 2015. Temperature responses of mesophyll conductance differ greatly between species. *Plant, Cell & Environment* **38**: 629-637.

von Caemmerer S, Farquhar GD. 1981. Some relationships between the biochemistry of photosynthesis and the gas exchange of leaves. *Planta* **153**: 376-387.

Wang YP, Leuning R. 1998. A two-leaf model for canopy conductance, photosynthesis and partitioning of available energy. I. Model description and comparison with a multi-layered model. *Agricultural and Forest Meteorology* **91:** 89-111.

Warren JM, Jensen AM, Medlyn BE, Norby RJ, Tissue DT. 2015. Carbon dioxide stimulation of photosynthesis in *Liquidambar styraciflua* is not sustained during a 12-year field experiment. *Aob Plants* **7**: plu074.

Way DA, Oren R, Kim H-S, Katul GG. 2011. How well do stomatal conductance models perform on closing plant carbon budgets? A test using seedlings grown under current and elevated air temperatures. *Journal of Geophysical Research: Biogeosciences* **116:** G4.

Way DA, Montgomery RA. 2015. Photoperiod constraints on tree phenology, performance and migration in a warmer world. *Plant, Cell & Environment* **38**: 1725-1736.

Way DA and Oren R. 2010. Differential responses to increased growth temperatures between trees from different functional groups and biomes: A review and synthesis of data. *Tree Physiology* **30:** 669-688.

Way DA, Yamori W. 2014. Thermal acclimation of photosynthesis: on the importance of adjusting our definitions and accounting for thermal acclimation of respiration. *Photosynthesis Research* **119:** 89-100.

Wilkinson S, Davies WJ. 2002. ABA-based chemical signalling: the co-ordination of responses to stress in plants. *Plant, Cell & Environment* **25:** 195–210.

Williams M, Rastetter EB, Fernandes DN, Goulden ML, Wofsy SC, Shaver GR, Melilo JM, Munger JW, Fan SM, Nadelhoffer KJ. 1996. Modelling the soil-plant-atmosphere continuum in a Quercus-Acer stand at Harvard forest: The regulation of stomatal conductance by light, nitrogen and soil/plant hydraulic properties. *Plant Cell & Environment,* **19**: 911-927.

Wright IJ, Reich PB, Westoby M, Ackerly DD, Baruch Z, Bongers F, Cavender-Bares J, Chapin T, Cornelissen JHC, Diemer M *et al*. 2004. The worldwide leaf economics spectrum. *Nature* **428:** 821-827.

Wu J, Albert LP, Lopes AP, Restrepo-Coupe N, Hayek M, Wiedemann KT, Guan K, Stark SC, Christoffersen B, Prohaska N, *et al*. 2016a. Leaf development and demography explain photosynthetic seasonality in Amazon evergreen forests. *Science* **351,** 972-976.

Wu J, Chavana-Bryant, C, Prohaska, N, Serbin, SP, Guan, K, Albert, L, Yang, X, van Leeuwen, W, Garnello, J, Martins, G, *et al*. 2016b. Convergence in relations among leaf traits, spectra and age across diverse canopy environments and two contrasting tropical forests. *New Phytologist* In Press. DOI: 10.1111/nph.14051.

Wullschleger SD, Epstein HE, Box EO, Euskirchen ES, Goswami S, Iversen CM, Kattge J, Norby RJ, van Bodegom PM, Xu X. 2014. Plant functional types in Earth system models: past experiences and future directions for application of dynamic vegetation models in high-latitude ecosystems. *Annals of Botany* **114,** 1-16.

Xu CG, Fisher R, Wullschleger SD, Wilson CJ, Cai M, McDowell NG. 2012. Toward a mechanistic modeling of nitrogen limitation on vegetation dynamics. *Plos One* **7**: e37914.

Yamori W, Hikosaka K, Way DA. 2014. Temperature response of photosynthesis in C_3, C_4, and CAM plants: temperature acclimation and temperature adaptation. *Photosynthesis Research* **119:** 101-117

Zaehle S, Friend AD. 2010. Carbon and nitrogen cycle dynamics in the O-CN land surface model: 1. Model description, site-scale evaluation, and sensitivity to parameter estimates. Global *Biogeochemical Cycles* **24**. GB1005.

Zaehle S, Medlyn BE, De Kauwe MG, Walker AP, Dietze MC, Hickler T, Luo YQ, Wang YP, El-Masri B, Thornton P *et al*. 2014. Evaluation of 11 terrestrial carbon-nitrogen cycle models against observations from two temperate Free-Air CO_2 Enrichment studies. *New Phytologist* **202:** 803–822.

Zhou SX, Duursma RA, Medlyn BE, Kelly JWG, Prentice IC. 2013. How should we model plant responses to drought? An analysis of stomatal and non-stomatal responses to water stress. *Agricultural and Forest Meteorology* **182**: 204-214.

Ziehn T, Kattge J, Knorr W, Scholze M. 2011. Improving the predictability of global CO_2 assimilation rates under climate change. *Geophysical Research Letters* **38**:L10404.

Figure Legends

Figure 1 The response of leaf level (a) and canopy level (b,c,d) photosynthesis (*A*) to instantaneous quantum flux density (*Q*) for three different values of leaf area index; LAI=1 (b), LAI=3 (c), and LAI=7 (d) for seven models; BETHY (red), CLM (blue), ED2 (cyan), JSBACH (pink), JULES (dark green) G'DAY (black), O-CN (green). Plots show responses in standard conditions for a single plant functional type, a generic temperate broad leaved deciduous tree. Where $V_{c,max}$ is 60 µmol m^{-2} s^{-1}. *VPD* was fixed at 1 kPa, soil moisture content was fixed at field capacity, and atmospheric [O_2] at 210 mmol mol^{-1}, C_a at 380 µmol mol^{-1}. Sunlit upper canopy leaf temperature was fixed at 25^{o}C.

Figure 2 The response of leaf level (a,b) and canopy level (LAI =3; c, d) photosynthesis (*A*) to leaf temperature at two atmospheric [CO_2] (380 µmol mol^{-1} a, c and 550µmol mol^{-1} b, d) for seven models; BETHY (red), CLM (blue), ED2 (cyan), JSBACH (pink), JULES (dark green) G'DAY (black), O-CN (green). Plots show responses in standard conditions for a single plant functional type, a temperate broad leaved deciduous tree. Where $V_{c,max}$ is 60 µmol m^{-2} s^{-1}. *VPD* was fixed at 1 kPa, soil moisture content was fixed at field capacity, and atmospheric [O_2] at 210 mmol mol^{-1}, *Q* at 1500 µmol m^{-2} s^{-1}. Sunlit upper canopy leaf temperature was fixed at 25^{o}C.

Figure 3 The response of leaf level (a,b) and canopy level (LAI=3; c,d) photosynthesis (*A*) to atmospheric [CO_2] (C_a) in seven models; BETHY (red), CLM (blue), ED2 (cyan), JSBACH (pink), JULES (dark green) G'DAY (black), O-CN (green). Panels show responses in our standard

conditions for a single plant functional type, a temperate broad leaved deciduous tree where $V_{c,max}$ = 60 µmol m^{-2} s^{-1} (a,c) and when $V_{c,max}$ = 45 µmol m^{-2} s^{-1} (b, d). The *VPD* was fixed at 1 kPa, soil moisture content at field capacity and *Q* at 1500 µmol m^{-2} s^{-1}, atmospheric [O_2] at 210 mmol mol^{-1} Sunlit upper canopy leaf temperature was fixed at 25°C.

Figure 4 The response of leaf level (a) and canopy level, where LAI=3 (b) photosynthesis (*A*) to vapor pressure deficit (*VPD*) for seven models; BETHY (red), CLM (blue), ED2 (cyan), JSBACH (pink), JULES (dark green) G'DAY (black), O-CN (green). Plots show responses in standard conditions for a common plant functional type, a temperate broad leaved deciduous tree. Where $V_{c,max}$ = 60 µmol m^{-2} s^{-1}. Soil moisture content was fixed at field capacity, *Q* at 1500 µmol m^{-2} s^{-1}, C_a at 380 µmol mol^{-1}, atmospheric [O_2] at 210 mmol mol^{-1} Sunlit upper canopy leaf temperature was fixed at 25°C.

Figure 5 The response of leaf level (a) and canopy level, where LAI=3 (b) photosynthesis (*A*) to soil water content expressed as a fraction of field capacity for seven models; BETHY (red), CLM (blue), ED2 (cyan), JSBACH (pink), JULES (dark green) G'DAY (black), O-CN (green). Plots show responses in standard conditions for a single plant functional type, a temperate broad leaved deciduous tree. Where $V_{c,max}$ = 60 µmol m^{-2} s^{-1}). *VPD* was fixed at 1 kPa, *Q* at 1500 µmol m^{-2} s^{-1}, C_a at 380 µmol mol^{-1}, atmospheric [O_2] at 210 mmol mol^{-1} Sunlit upper canopy leaf temperature was fixed at 25°C.

Figure 6 Summary of the main areas of scientific activity required to advance representation of photosynthesis in Earth System Models. Blue boxes show areas where fundamental research is required to advance understanding prior to incorporation into models. Yellow boxes show areas where model refinement or development is required to improve process representation. Green boxes highlight areas where data are needed to parameterize models or are required to evaluate alternative approaches. The numbers in the boxes are keyed to our recommendations in the text.

Table 1 Model representation of the response of C_3 photosynthesis to key environmental variables used for this study.

BETHY	CLM4.5	ED2	G'DAY	JSBACH	JULES	O-CN
Leaf photosynthesis (response to C_a)						
Farquhar et al (1980), no TPU limitation	Farquhar et al (1980), includes TPU limitation and co-limitation from Collatz et al. (1991)	Collatz et al. (1991) and Foley et al. (1996); no TPU limitation	Farquhar et al (1980), no TPU limitation	Farquhar et al (1980), no TPU limitation	Collatz et al. (1991), TPU limitation included	Farquhar type (Farquhar et al 1980) following Kull and Kruijt (1998)
Stomatal conductance (response to atmospheric *VPD*, C_a soil moisture and *A*)						
Minimum of (1) stomatal conductance necessary to realize maximum C_i:C_a and (2) soil water availability (Federer 1982).	Sensitivity to atmospheric *RH*, C_a and *A* from Ball, Woodrow & Berry (1987) Sensitivity to soil moisture is from a beta factor applied to the intercept of the Ball, Woodrow & Berry (1987) model. The beta factor is summed over soil layers, weighted by root fraction in each layer and calculated based on soil moisture content	Sensitivity to atmospheric *VPD*, C_a and *A* from Leuning et al. (1995) Water supply is proportional to soil moisture root biomass. If the open stomata demand exceeds supply then g_s is linearly scaled between open and closed stomata.	Sensitivity to atmospheric *VPD*, C_a and *A* from Medlyn et al. (2011) Sensitivity to soil moisture from beta factor applied to the slope of the stomatal response (Medlyn et al. 2011). Soil moisture content is expressed as a fraction of total plant available water and dependent on soil type	Estimates potential *A* for any given condition assuming a maximal C_i:C_a resulting from a maximum potential g_s When soil moisture content falls below 50% of plant available water maximum potential g_s is reduced linearly.	Sensitivity to atmospheric *VPD*, C_a and *A* from modification of Leuning et al (1995) model as proposed by Jacobs (1994)	Non-linear sensitivity to specific humidity deficit and C_i. The latter is necessary because *A* for g_s is evaluated at saturating C_i. A beta factor is applied to the slope of the stomatal response when soil moisture content falls below 50% of plant available water.
Leaf photosynthesis (response to light)						
Rectangular hyperbola, with realized quantum yield and A_{sat} calculated from Farquhar model	Non-rectangular hyperbola, with realized quantum yield and A_{sat} calculated from Farquhar model	Hyperbolic function, with realized quantum yield and A_{sat} calculated from the Collatz (1991) model, no J_{max} term included	Non-rectangular hyperbola, with realized quantum yield and A_{sat} calculated from Farquhar model	Rectangular hyperbola, with realized quantum yield and A_{sat} calculated from Farquhar model	Hyperbolic function, with realized quantum yield and A_{sat} calculated from the Collatz (1991) model, no J_{max} term included	Explicit separation into light saturated and limited regions: A_{sat} is calculated from Farquhar et al (1980). Light

						limited A is assumed to be proportional to light absorption (Kull and Kruijt, 1998)
Leaf photosynthesis (response to temperature)						
Temperature dependence of kinetic constants follows Bernacchi et al. (2001). $V_{c,max}$ and J_{max} are peaked Arrhenius functions of temperature.	Temperature dependence of kinetic constants follows Bernacchi et al. (2001). $V_{c,max}$ and J_{max} are peaked Arrhenius functions of temperature. TPU has the same temperature response as V_{cmax}.	Follows Collatz et al., (1991) and Foley et al., (1996). The temperature dependent kinetic constants follow a modified Arrhenius function. A phenomenological thermal downscaling of $V_{c,max}$ occurs at low and high temperatures (Medvigy et al., 2009)	Temperature dependence of kinetic constants follows Bernacchi et al. (2001). $V_{c,max}$, J_{max} and R_d are peaked Arrhenius functions (Medlyn et al. 2002).	Temperature dependence of kinetic constants and $V_{c,max}$ follow an Arrhenius function, Γ* and J_{max} vary linearly with temperature.	Follows Collatz et al. (1991), the temperature dependence of kinetic constants follows a Q_{10} function. $V_{c,max}$ has a peaked temperature function calculated from $V_{c,max}$ at 25°C using vegetation-specific optimal temperature ranges.	Temperature dependence of kinetic constants and $V_{c,max}$ follows Bernacchi et al. (2001). The temperature dependence of J_{max} is derived from June et al. (2004)
Leaf photosynthesis (response to soil moisture content)						
	A beta factor is applied to $V_{c,max}$. The beta factor, calculated based on soil moisture potential, is summed over soil layers, weighted by root fraction in each layer.		A beta factor is applied to J_{max} and $V_{c,max}$. Soil moisture content is expressed as a fraction of total plant available water and dependent on soil type		Potential A is multiplied by a soil water stress factor related to the mean soil moisture concentration in the root zone and the critical and wilting point soil water concentrations.(Cox et al.,1998)	A beta factor reduces $V_{c,max}$ and J_{max} when plant available water <20% (Friend, 2010)
Canopy scaling						
Multiple canopy	The Multi-layer	Cohort-based model	Big-leaf model,	Multiple canopy	Multi-layer canopy	Multiple canopy

layers, using Sellers's (1987) two-stream approximation. $V_{c,max}$ and J_{max} declines exponentially within the canopy following Lloyd et al. (2012).	option explicitly resolves direct and diffuse radiation for sunlit and shaded leaves at each level in the canopy. Both options use Sellers's (1987) two-stream approximation for radiative transfer. Nitrogen declines exponentially with greater cumulative leaf area index.	with the number of layers equal to the number of cohorts. Cohorts differ by PFT definition. Radiation penetration is defined by LAI and the leaf and wood single scattering albedos. There is no separation of sunlit and shaded foliage in the default version	assuming exponential light and nitrogen distributions. Daily *A* calculated using Gaussian integration (Sands 1996)	layers, using Sellers's (1987) two-stream approximation. LAI typically = 3. For LAI < 3, N (and hence $V_{c,max}$, J_{max}) is distributed evenly in the canopy (assumed to be open). For LAI > 3, N follows the distribution of light (exponential decline).	using the two-stream approximation from Sellers (1985) solving direct and diffuse radiation for sunlit and shaded leaves at each canopy layer. Includes exponential vertical nitrogen distribution of photosynthetic capacity and leaf respiration.	layers with diffuse and direct radiation streams following Spitters (1986). Nitrogen declines exponentially with greater cumulative leaf area index, affecting $V_{c,max}$ and J_{max}
Key Model References						
Knorr & Heimann (2001)	Bonan et al (2011, 2012), Oleson et al (2013)	Medvigy et al (2009), Moorcroft et al (2001)		Knorr & Heimann (2001)	Best et al (2011), Clark et al (2011), Harper (2016)	Zaehle & Friend (2010), Friend (2010)

BETHY = Biosphere Energy Transfer Hydrology scheme, CLM4.5 = the Community Land Model version 4.5, G'DAY = Generic Decomposition And Yield model (G'DAY), JSBACH = Joint Scheme for Biosphere Atmosphere Coupling in Hamburg, JULES = Joint UK Land Environment Simulator, O-CN = An extension of the Organizing Carbon and Hydrology in Dynamic Ecosystems model that includes key N cycle processes.

Table 2 Parameters used by the models in this study (Table 1).

	BETHY	CLM4.5	ED2	G'DAY	JSBACH	JULES	O-CN
K_c at 25°C (µmol mol^{-1})	404.9	404.9	300	404.9	404.9	300	404.9
K_o at 25°C (mmol mol^{-1})	278.4	278.4	294	278.4	278.4	300	278.4
Γ^* at 25°C (µmol mol^{-1})	42.75	42.75	41.57	42.75	42.75	40.38	42.75
Source of kinetic constants	Bern	Bern	Foley	Bern	Bern	Collatz	Bern
JV_{ratio}	1.92	1.97	N.A.	2.00	1.90	N.A.	2.08
J_{max} (µmol m^{-2} s^{-1})	115(86)	115(85)	N.A.	120(90)	114(86)	N.A.	126(94)
Absorbtance	0.88	0.85	0.73	0.85	0.88	0.85	0.80
Convexity	N.A.	0.98 & 0.95[a]	N.A.	0.7	N.A.	0.83 & 0.93[a]	N.A.
C_i at low light (µmol mol^{-1})	348	400	400	293	348	280	N.D.
Model input for quantum yield	0.28[b]	0.4250[b]	0.08[d]	0.26[c]	0.28[b]	0.08[d]	0.08[d]
Calculated ϕ_{int}	0.070	0.106	0.080	0.076	0.070	0.080	0.080
ϕ_{real}	0.049	0.053	0.038	0.038	0.050	0.045	0.022

The Michaelis-Menton constants of Rubisco for carbon dioxide (K_c) and oxygen (K_o), the CO_2 compensation point in the absence of non-photorespiratory michondrial respiration in the light (Γ^*) and the sources of those kinetic constants (Bern = Bernacchi et al. 2001, Collatz = Collatz et al. 1991, Foley = Foley et al. 1996). Where applicable the model specific ratio of the maximum electron transport rate (J_{max}) to maximum photosynthetic capacity ($V_{c,max}$), the (JV_{ratio}), was used to calculate J_{max} for standard conditions, low nitrogen conditions are shown in parentheses. Leaf absorbtance; the convexity term ([a]for the transition between Rubisco and light limited and light limited and TPU limited A respectively); the intercellular [CO_2] (C_i) at low light. Three model inputs were used to parameterize quantum yield ([b]quantum yield of electron transport based on absorbed light, [c]quantum yield of electron transport based on incident light and [d]quantum yield of photosynthesis based on absorbed light and measured under non-photorespiratory conditions (ϕ_{int}). Here we also show the calculated intrinsic quantum yield for all models to enable model comparisons. The modeled realized quantum yield under our standard conditions when Q = 100 µmol mol^{-1} (ϕ_{real}) is the initial slope of the leaf level A-Q response shown in Fig 1a for our standard conditions where the ($V_{c,max}$) was set to 60 µmol m^{-2} s^{-1} (and 45 µmol m^{-2} s^{-1} for low nitrogen conditions) and where temperature = 25°C, atmospheric [O_2] = 210 mmol mol^{-1}, C_a = 380 µmol mol^{-1}, VPD = 1 kPa and soil moisture content was at field capacity. N.A. = not applicable, N.D. = no data.

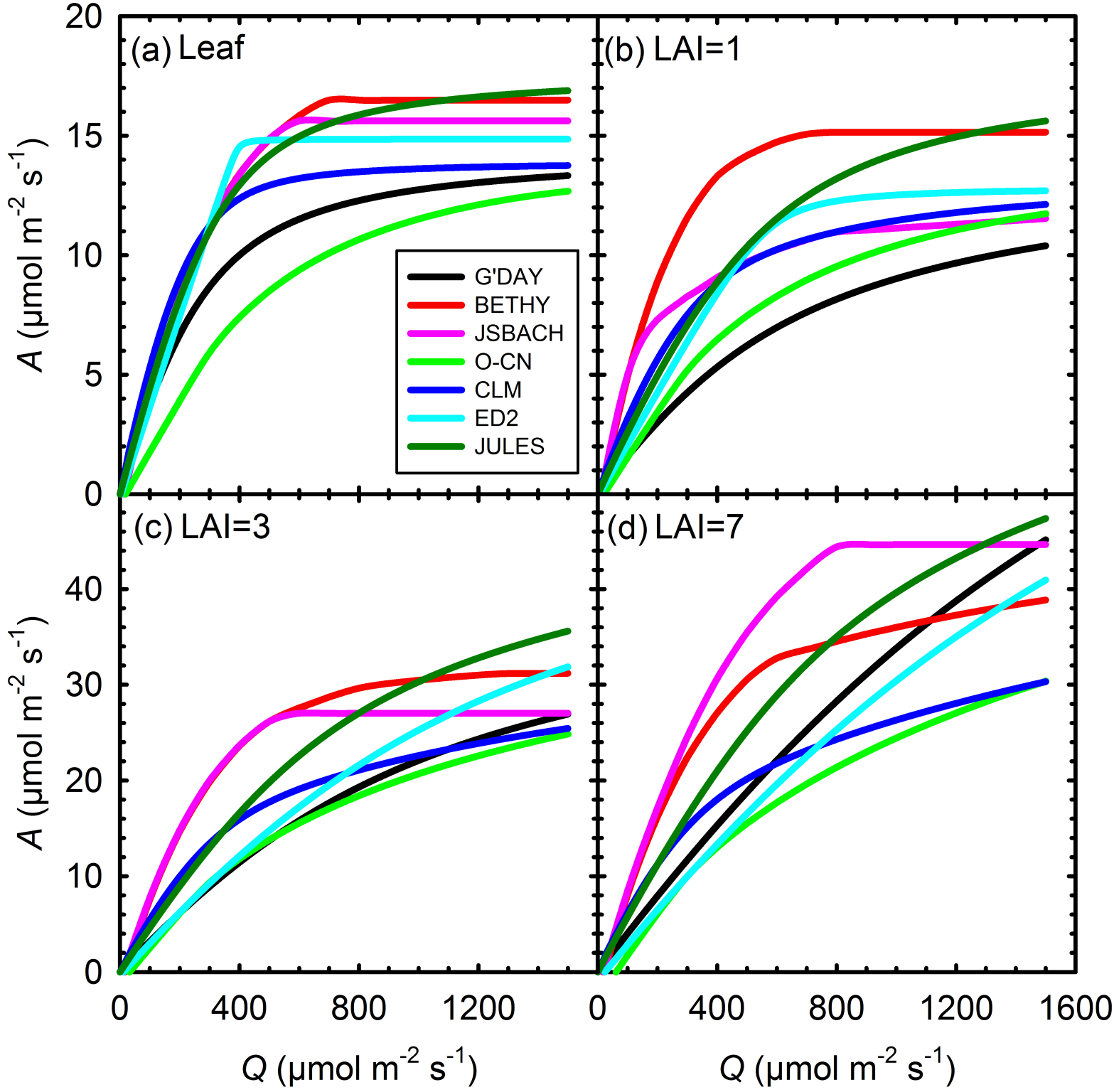
(a) Leaf
(b) LAI=1
(c) LAI=3
(d) LAI=7
G'DAY
BETHY
JSBACH
O-CN
CLM
ED2
JULES
A (μmol m-2 s-1)
Q (μmol m-2 s-1)
0
5
10
15
20
30
40
400
800
1200
1600

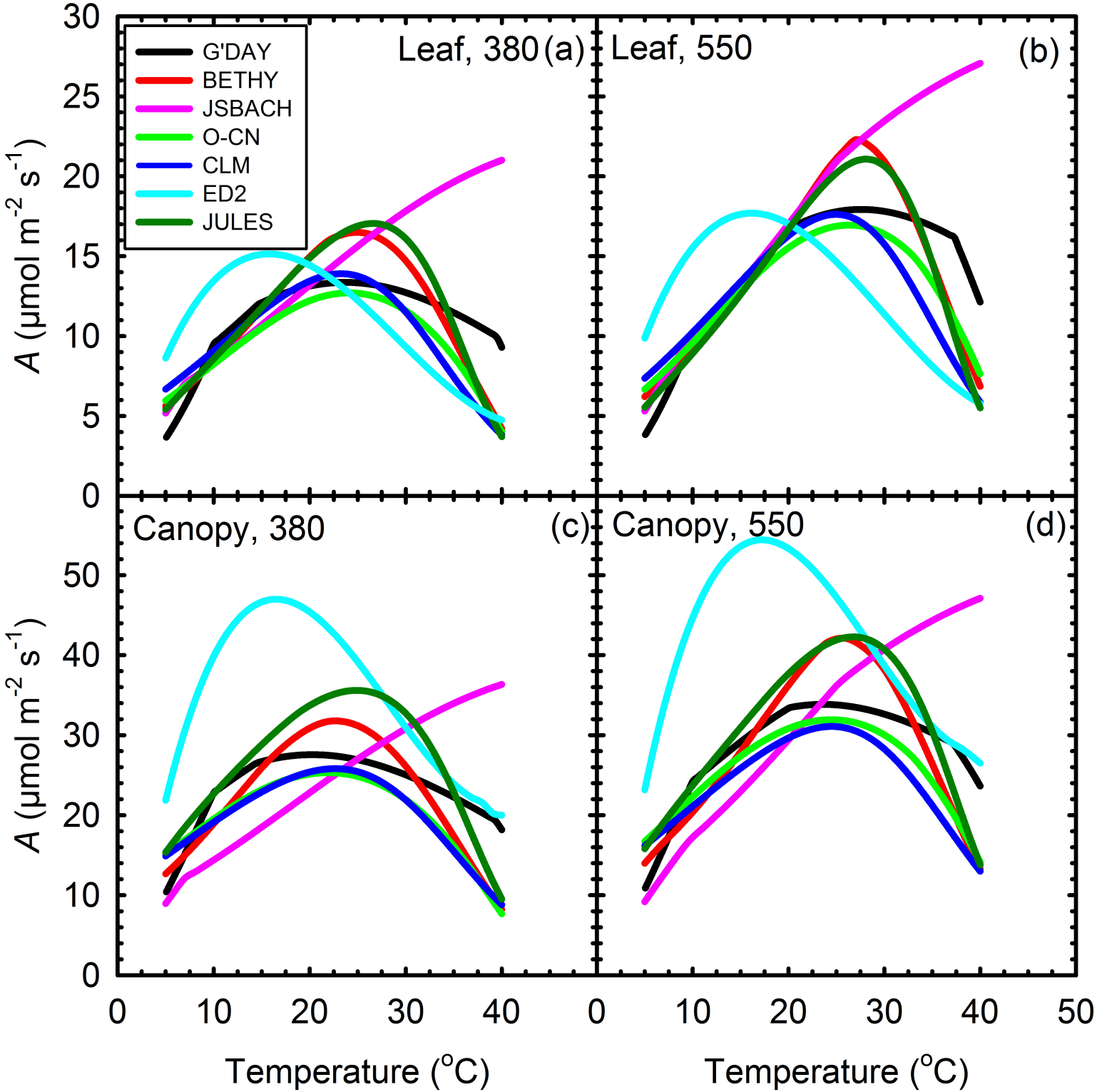
G'DAY
BETHY
JSBACH
O-CN
CLM
ED2
JULES
Leaf, 380
(a)
Leaf, 550
(b)
Canopy, 380
(c)
Canopy, 550
(d)
A (μmol m-2 s-1)
A (μmol m-2 s-1)
Temperature (°C)
Temperature (°C)
0
5
10
15
20
25
30
0
10
20
30
40
50
0
10
20
30
40
0
10
20
30
40
50

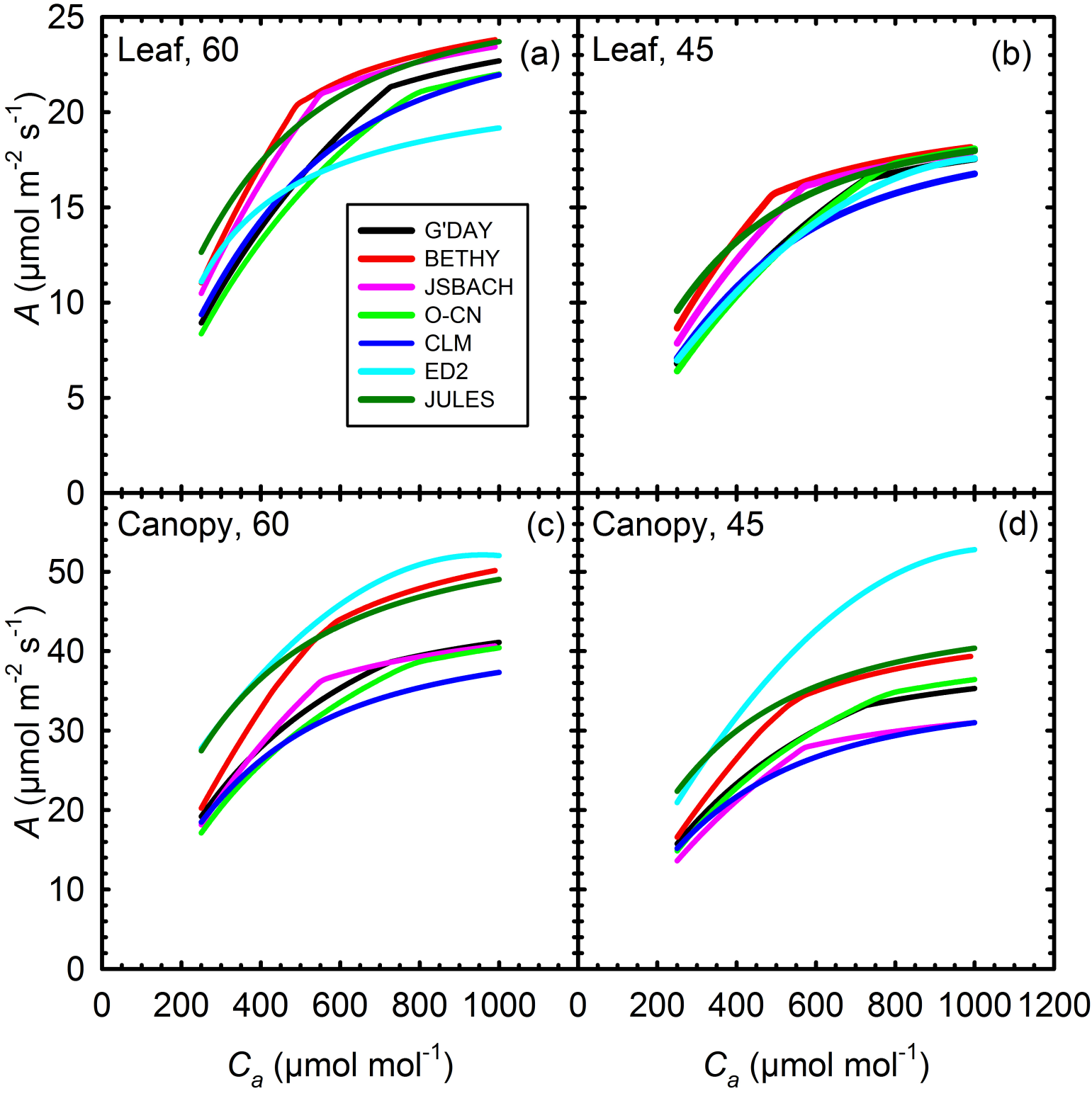
Leaf, 60
(a)
Leaf, 45
(b)
Canopy, 60
(c)
Canopy, 45
(d)
G'DAY
BETHY
JSBACH
O-CN
CLM
ED2
JULES
A (μmol m-2 s-1)
Ca (μmol mol-1)
0
5
10
15
20
25
30
40
50
200
400
600
800
1000
1200

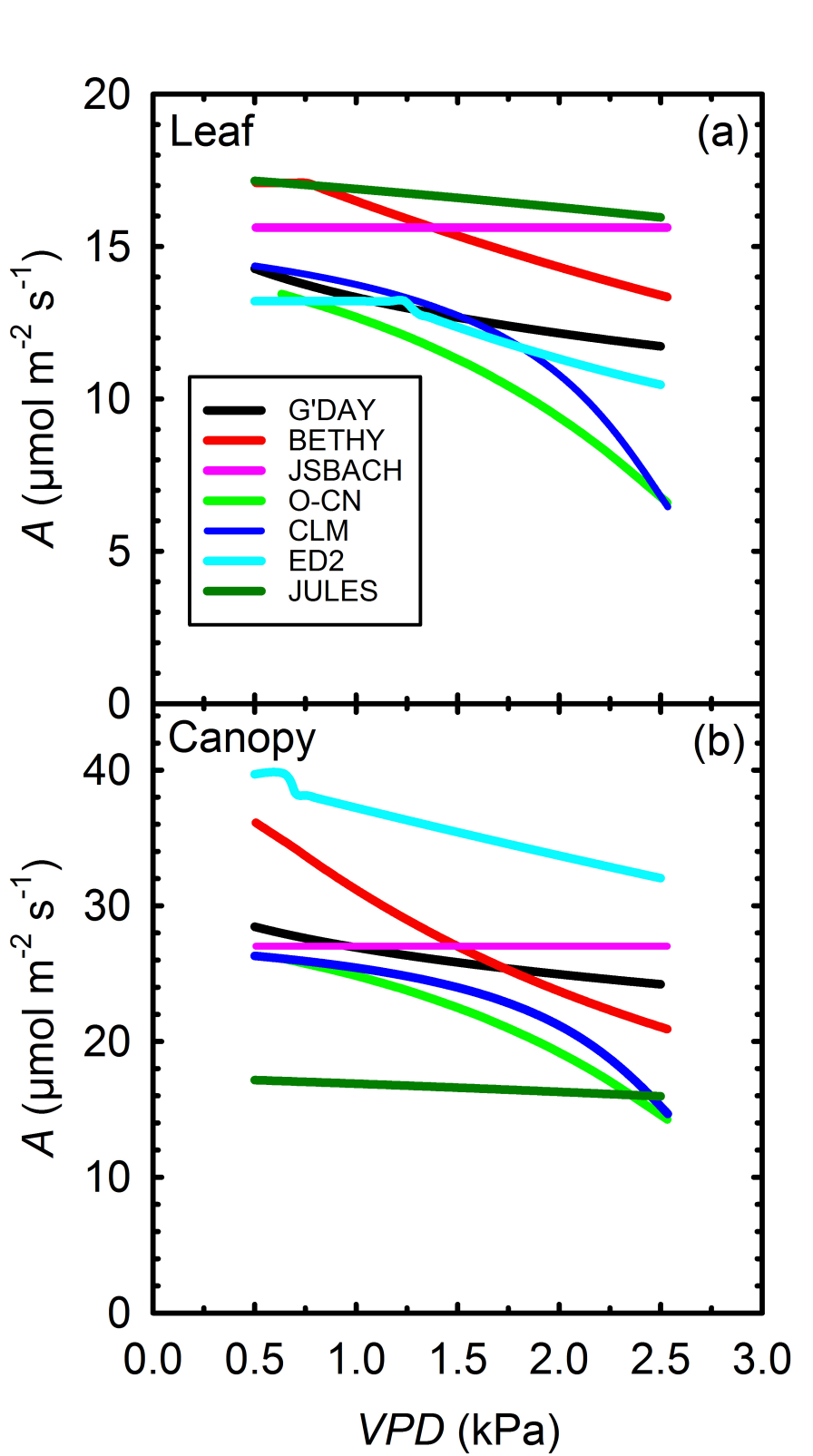
Leaf
(a)
Canopy
(b)
A (μmol m-2 s-1)
VPD (kPa)
G'DAY
BETHY
JSBACH
O-CN
CLM
ED2
JULES
0
5
10
15
20
0
10
20
30
40
0.0
0.5
1.0
1.5
2.0
2.5
3.0

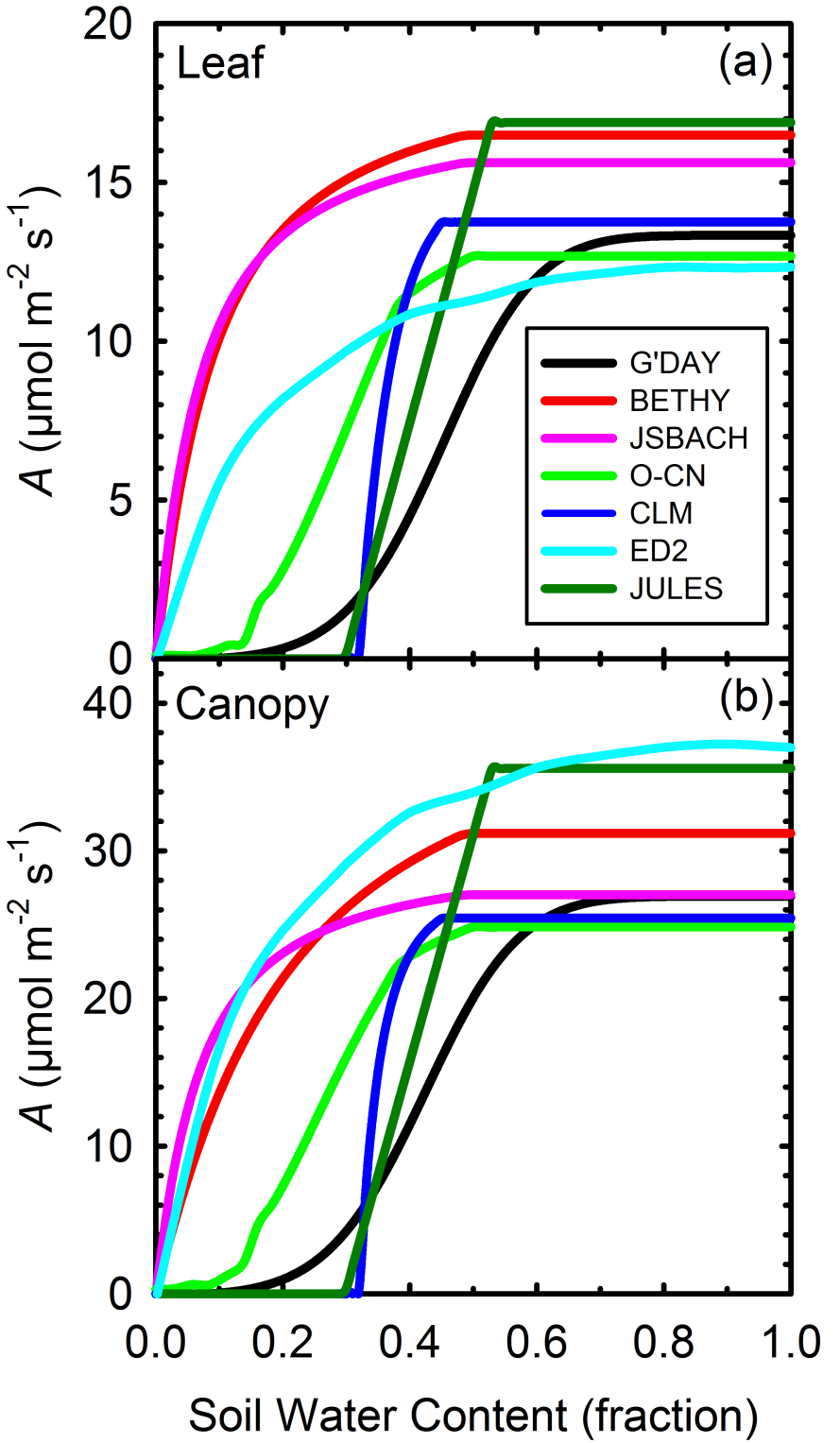
Leaf
(a)
Canopy
(b)
A (μmol m-2 s-1)
Soil Water Content (fraction)
G'DAY
BETHY
JSBACH
O-CN
CLM
ED2
JULES
0
5
10
15
20
30
40
0.0
0.2
0.4
0.6
0.8
1.0

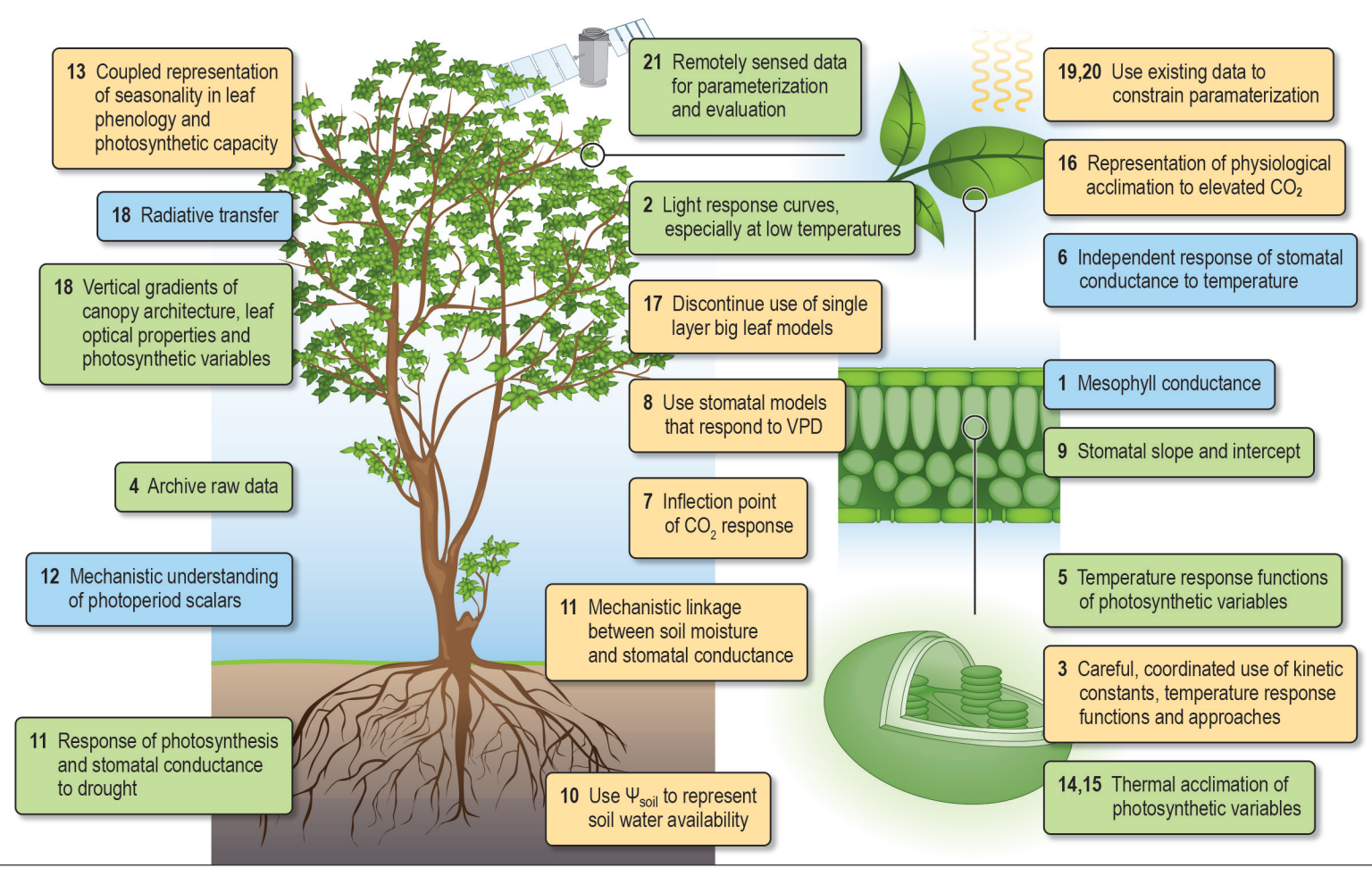
13 Coupled representation of seasonality in leaf phenology and photosynthetic capacity
18 Radiative transfer
18 Vertical gradients of canopy architecture, leaf optical properties and photosynthetic variables
4 Archive raw data
12 Mechanistic understanding of photoperiod scalars
11 Response of photosynthesis and stomatal conductance to drought
21 Remotely sensed data for parameterization and evaluation
2 Light response curves, especially at low temperatures
17 Discontinue use of single layer big leaf models
8 Use stomatal models that respond to VPD
7 Inflection point of CO_2 response
11 Mechanistic linkage between soil moisture and stomatal conductance
10 Use Ψ_{soil} to represent soil water availability
19,20 Use existing data to constrain paramaterization
16 Representation of physiological acclimation to elevated CO_2
6 Independent response of stomatal conductance to temperature
1 Mesophyll conductance
9 Stomatal slope and intercept
5 Temperature response functions of photosynthetic variables
3 Careful, coordinated use of kinetic constants, temperature response functions and approaches
14,15 Thermal acclimation of photosynthetic variables
Data needed for model parameterization or evaluation
Model development activity
Process knowledge required